Carbonates Evaporites (2019) 34:315–334
DOI 10.1007/s13146-017-0387-9

ORIGINAL ARTICLE

Paleogeographic evolution of the Maastrichtian deposits in the eastern Fars area (Zagros, Iran) using high-resolution sequence stratigraphic analysis

S. Parham[1] · A. R. Piryaei[2] · M. Ghorbani[1] · R. Moussavi-Harami[3]

Accepted: 12 August 2017 / Published online: 27 October 2017

Abstract Upper Cretaceous depositional systems of the Zagros area were influenced by a series of local and regional tectono-sedimentary events such as progressively southwestward foreland basin migration, which locally was overprinted by salt movements. The Maastrichtian interval is characterized by filling out of the NE foredeep by obducted units and development of SW facing ophiolitic and radiolite nappe in the most interior parts of the Fars area. This tectono-sedimentary loading led to the migration of the mid-foreland basin bulge to the southwest. To reconstruct the depositional settings during this time, three outcrop sections (Kuh-e Chadur, Gach, and Parak) and two wells (Pishvar-1 and Bavush-1) are organized in an SW–NE trending cross section. Maastrichtian sedimentary succession is introduced by pelagic marls of the Gurpi Formation, carbonates of the Tarbur, and evaporates of the Sachun formations along with obducted radiolaritic and ophiolitic complexes. Field and microscopic investigations led to the recognition of several facies' belts in carbonate domain including intertidal, restricted and open lagoonal, reefal, open marine, and basinal settings, which organized in one regional third- and five local fourth-order sequences that generally show a sharp decreasing trend in sequence thickness of Maastrichtian deposits from NE toward SW. Facies' variations along this transect show that sequences 1 and 2 are present only in the northern part of the basin. Sequence 3 dominated by rudistid facies, showing progradational pattern toward the southern basinal setting over the time-equivalent pelagic marls of the Gurpi Formation. Sequence 4 has mainly composed of inner shelf deposits in the north and progrades into the outer shelf deposits, toward the south. Sequence 5 consists mainly of dolomites and evaporites of restricted lagoon (Sachun Formation). Accordingly, salt tectonics has resulted in thickness and facies' variations as well as sequence patterns. In addition, uplifting and migration of the bulge, controlled the exposure area and subsequent diagenetic events such as meteoric dissolution, dolomitization, neomorphism, brecciation, and Fe-staining. Halokinetic events show a strong influence on the intensity and development of diagenetic processes, particularly dolomitization and dissolution.

Keywords Maastrichtian · Eastern Fars · Zagros · Foreland basin · Depositional setting · Sequence stratigraphy

Introduction

The most significant tectono-sedimentary event of the NE margin of Arabian Plate (including the eastern Fars area) during the Late Cretaceous is characterized by development and migration of the foreland basin to the SW which was associated by changes in depocenters as well as basinal and platformal settings (Alavi 2007; van Buchem et al. 2006; Piryaei et al. 2010, 2011). This process could be due to stack thrusting and subsequent tectono-sedimentary loading in the northern side of the foreland basin. Salt

✉ S. Parham
parhams@ripi.ir

[1] Department of Geology, Faculty of Sciences, Hormozgan University, Bandar Abbas, Iran

[2] National Iranian Oil Company, Exploration Directorate, Tehran, Iran

[3] Department of Geology, Faculty of Sciences, Ferdowsi University of Mashhad, Mashhad, Iran

tectonics also locally affected the sedimentary systems (Player 1967; Kent 1970; Jahani et al. 2007, 2009). These changes in depositional features can be traced in the Maastrichtian sequences of the eastern Fars area. This time interval includes the upper part of Gurpi, Tarbur and lower part of Sachun formations as well as obducted radiolarite and ophiolitic complex. In terms of stratigraphy and regional paleogeography, many works have been published by authors (e.g., James and Wynd 1965; Setudenia 1978; Koop and Stoneley 1982; Amiri Bakhtiar et al. 2011; Pir-yaei et al. 2010, 2011; Abyat et al. 2013, 2015; Asgari Pirbalouti et al. 2012, 2013; Afghah and Yaghmour 2014). Despite this good background, little is known about the palaeogeographic evolution of eastern Fars area during and in relation with the Late Cretaceous tectonic and structural evolutions. The main goal of this paper is to interpret and map the migration effects of this foreland basin. To investigate Maastrichtian paleogeographic evolution, an SW–NE trending regional transect has been selected perpendicular to the Zagros main thrust, passing through the Kuh-e Chadur, Kuh-e Gach, and Kuh-e Parak outcrop sections together with subsurface data from the Pishvar-1 and Bavush-1 wells (Fig. 1). High-resolution sequence stratigraphic framework is prepared to understand the regional and local tectonic influences on the Maastrichtian sedimentary systems of the study area.

Materials and methods

A total of 400 thin sections have been studied from three outcrop sections and two exploration wells. Petrographic studies and microscopic image analyses were carried out on thin sections. The modified Dunham (1962) textural scheme of Embry and Klovan (1971) was used for facies' classification. In addition, field observations have been done to follow the bedding patterns and geometries, facies and thickness variations, and sequence stratigraphic surfaces and system tracts. Well data include paleontological range charts and biozonation, lithological interpretations associated with gamma ray and sonic logs. Based on this information, microfacies, depositional environments, and sequence stratigraphic framework reconstructed for the Maastrichtian sedimentary sequences. A combination of field observations, microscopic results and well log interpretation is used to understand the tectono-sedimentary evolution of eastern Fars area during the studied time interval. Dating of depositional sequences and sequence surfaces is based either on the Wynd's (1965) biozonation or log correlation in the dolomitic intervals or other barren units. Depositional environment was studied based on the standard facies' models presented by Wilson (1975) and Flügel (2010) standard models and sequence stratigraphic approach of van Wagoner et al. (1988), Vail (1991), Tucker

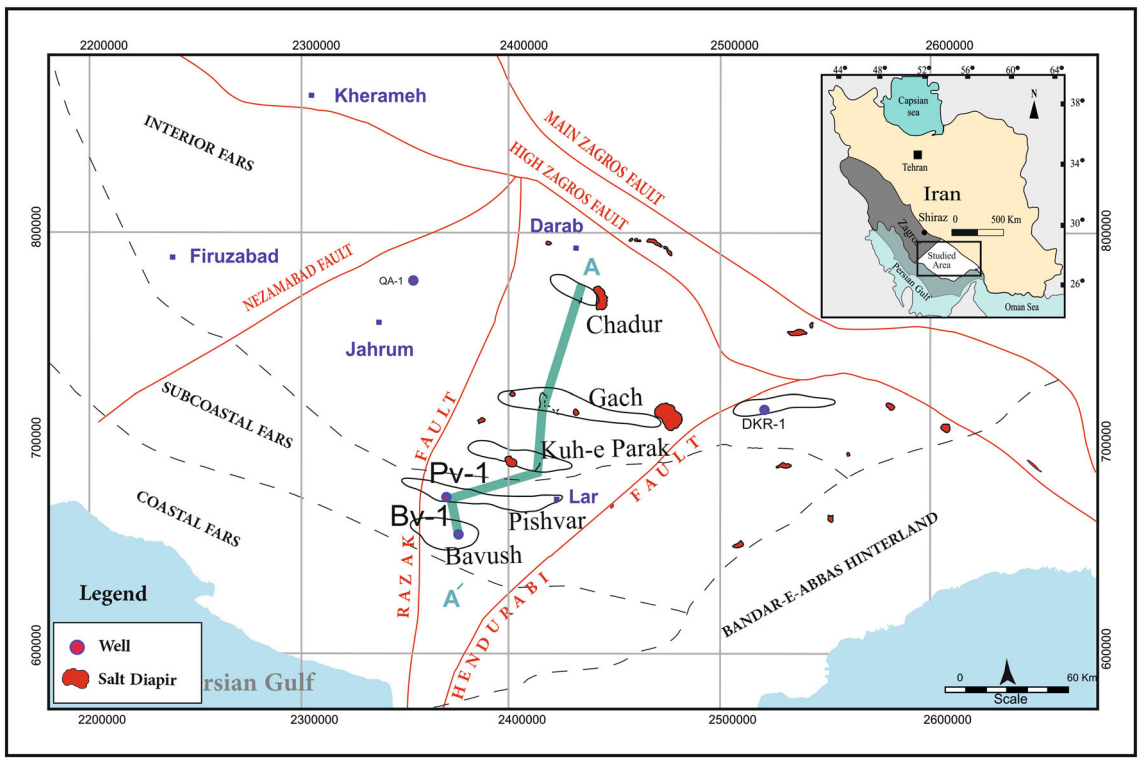

Fig. 1 Location map of the studied area showing the selected transect in the eastern part of the Fars area

(1993) and Emery and Myers (1996) Catuneanu et al. (2011, 2012) methods.

Geological setting

The study area covers mostly the interior parts of the Fars area, an area between the Nezam Abad Fault to the west and Bandar Abbas region to the east (Fig. 1). The Fars area is a part of the Zagros Foreland Fold and Thrust Belt (FFTB), belonging to the northeastern margin of the Arabian Plate (Alavi 2004; van Buchem et al. 2002; Piryaei et al. 2010, 2011). In addition to plate-scale foreland basin formation and obduction along the NE Zagros FFTB, Fars area also hosts many halokinetic events that episodically influenced the accommodation space and subsequent facies and thickness variations. A transect selected for this study that passes across the interior and sub-coastal Fars areas (Fig. 1).

Salt diapirs and Nezam Abad, Razak, Hendurabi, and High Zagros faults are important tectonic elements of the Fars area. These tectonic features strongly affect the sedimentation patterns of this area (Hesami et al. 2001; Bahroudi and Koyi 2003; Sepehr and Cosgrove 2005; Piryaei et al. 2010, 2011).

Salt tectonics occurs throughout the southeastern Zagros, as salt plugs exposed at the surface (e.g., at the Korsia, Gach, and Khamir anticlines) and/or known from the subsurface (e.g., the Genow anticline). Salt in the diapirs originates from the Infracambrian Hormuz Series and the Miocene Gachsaran Formation (Harrison 1930; Motiei 1995; Talbot and Alavi 1996; Ghazban and Al-Aasm 2010; Motamedi et al. 2011), both of which act as detachment horizons throughout the Zagros (Kent 1958, 1979; Sherkati and Letouzey 2004; Jahani et al. 2007).

Stratigraphy

The main Maastrichtian lithostratigraphic units of the studied area are the upper part of Gurpi, Tarbur and the lower part of the Sachun formations and emplaced radiolarites which are briefly discussed in the following (Fig. 2).

Gurpi Formation The Santonian-to-Maastrichtian Gurpi Formation is dominated by thin-bedded pelagic marls which locally prograded by time equivalent carbonate facies of the Tarbur Formation in its upper part. This basinal facies is resting unconformably on the Albian-to-Santonian Sarvak-to-Ilam formations. Depending on the tectono-sedimentary setting, thickness of the Gurpi Formation varies from a few meters to more than one thousand meter and wedges out toward the paleohighs. The Gurpi Formation is found almost throughout of southwestern Iran and extends from Fars region and parts of the Dezful Embayment area and from the Campanian to Paleocene in the Lurestan.

Tarbur Formation The Tarbur Formation consists of a thick carbonate sequences with Late Companian-to-Maastrichtian age. The basal contact of this formation in the northern part of the Zagros (Darab area) with radiolarites is sharp (Fig. 3a) and in other parts of the basin with the Gurpi Formation is conformable and transitional (Fig. 3b). The upper contact with the grey to green, ferruginous shales of the Sachun Formation is associated with ironstone nodules which may indicate an interruption in sedimentation process. Toward the southwest of area, the Tarbur Formation grades into shales of the Gurpi Formation (James and Wynd 1965; Ghazban 2009).

Sachun Formation The uppermost Maastrichtian-to-Paleocene Sachun Formation comprises a variety of lithologies including intercalation of dolomite and evaporite, dolomitic limestone, argillaceous dolomite, shale, marl, and clastics. Toward southwest, this formation changes to Pabdeh Formation. In the northern part of the Fars area (Kuh-e Ahmadi and Mozaffari), the Sachun Formation is divided to members including Qorban limestone and Sarvestan (Motiei 1993). The Sachun Formation is restricted to the northeastern interior Fars of the Zagros Fold-Trust Belt. It also presents in northwest of Bandar Abbas (Finu and Kuh-e Namak), east of Shiraz (Sarvestan) and Burkh, Bavush, and Darmadan (James and Wynd 1965; Motiei 1993). The thickness of this formation increased from southwest to southeast.

Regional sedimentary facies' distribution

The sedimentary facies and diagenetic processes can be attributed to two different tectono-sedimentary settings; a migrating platformal setting related to the foreland basin bulge and salt-induced facies and diagenetic features. Maastrichtian deposits consist of large variety of skeletal and non-skeletal grains. Skeletal components include *Omphalocyclus macroporus*, *Loftusia* sp., echinoids, *Siderolites calcitrapoides*, *Orbitoides* sp., sponge spicule and planktonic foraminifera such as *Globotruncana* sp., *Globotruncana stuarti,* and *Heterohelix* sp. Non-skeletal grains mainly consist of peloids and intraclasts. Based on the microscopic results and field observations including the study of sedimentary textures and structures, faunal assemblage, diagenetic features, and bedding patterns, different microfacies have been identified in the studied interval which can be classified into six facies' belts.

Tidal flat facies' belt

Tidal flat facies are mainly distributed in the northern part of the study area (e.g., Kuh-e Chadur section), where open

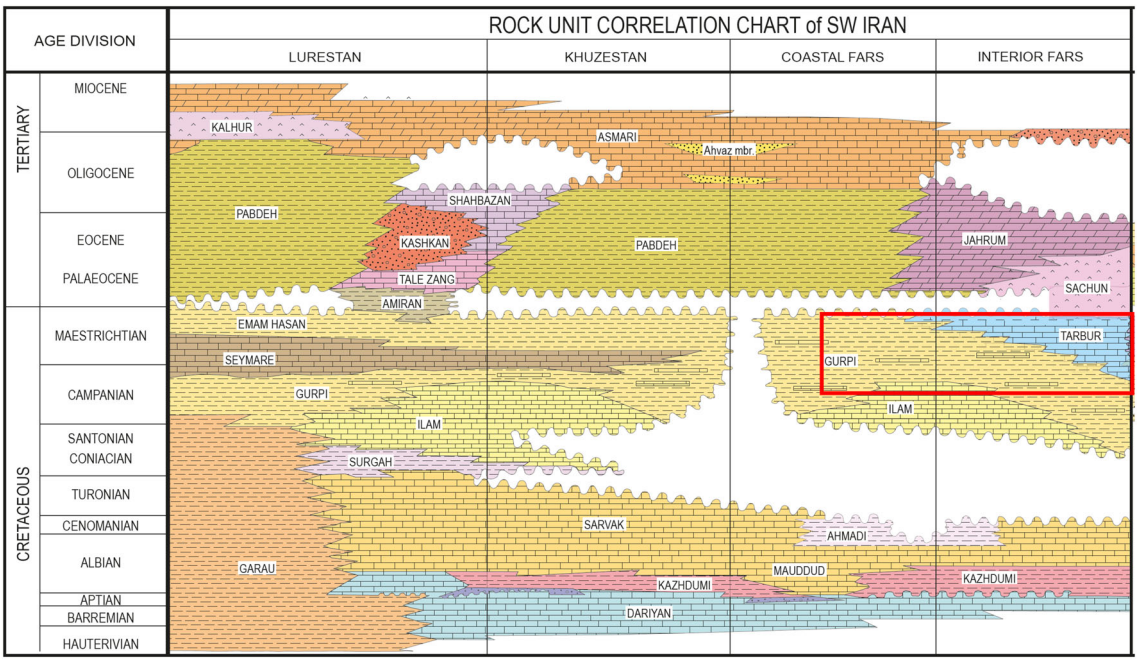

Fig. 2 Lithostratigraphic correlation chart of Zagros (after James and Wynd 1965; Motiei 1993). The studied interval includes the Maastrichtian Tarbur, Gurpi, and Sachun formations

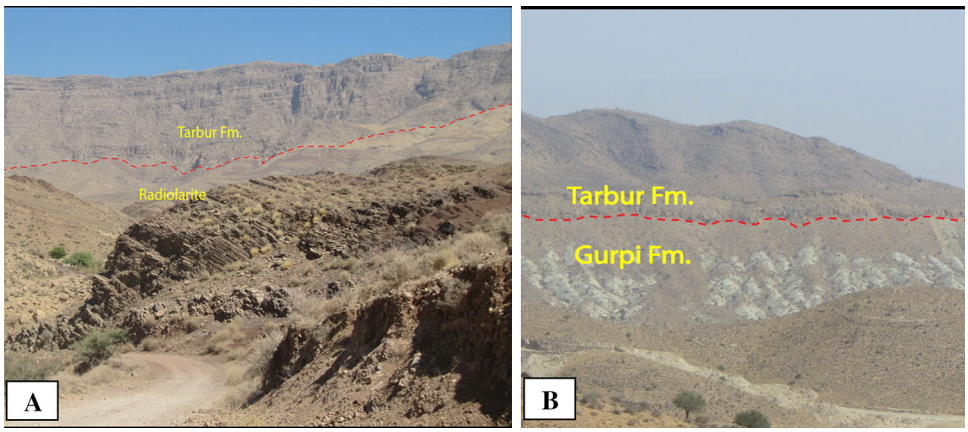

Fig. 3 **a** Field photos of the Tarbur Formation with obducted radiolarites, Barfdun Anticline, Darab area. **b** Filed photos of transitional contact of Tarbur–Gurpi formations. Mozaffari Anticline, south Shiraz

platform environments are turning to restricted and marginal environments (a transition from the Tarbur bioclast dominated facies to evaporitic Sachun facies). These facies include: A1-Coarse-grained intraclast rudstone associated with other non-skeletal grains such as peloid and oncoid, which is deposited in intertidal to supratidal and high energy environments and can be equivalent to SMF 24 of Flügel (2010) (Fig. 4a). A2-Dolomudstones (Fig. 4b) with fenestral fabric in which the size of dolomitic crystals reaches to about 2 micron and is equivalent to SMF 25 of Flügel (2010). A3-Ooid packstone (200 micron in size) with bioclastic cores and mostly superficial texture. This type of facies is interpreted to be deposited in tidal channel and shows an inversional texture partly dolomitization (Fig. 4c). A4-Stromatolite bindstone associated with mud cracks and tepee structures, mould of evaporitic minerals, silt-sized quartz grains, and algal filaments (Fig. 4d). The stromatolite laminae are planar and locally wavy and are attributed to supratidal to upper intertidal environment (Tucker and Wright 1990; Flügel 2010). This microfacies is equivalent to SMF 20 of Flügel (2010).

Restricted lagoonal facies' belt

Two microfacies have been identified in this facies belt: B1-Dolomitized bioclast peloid packstone and wackestone with micritized bioclasts (~20–40%) and common bioturbation (Fig. 4e) and B2-Dacyclad bioclast packstone with green algae, miliolids, textularids and 40–60% peloid. This microfacies is completely dolomitized (Fig. 4f). It is

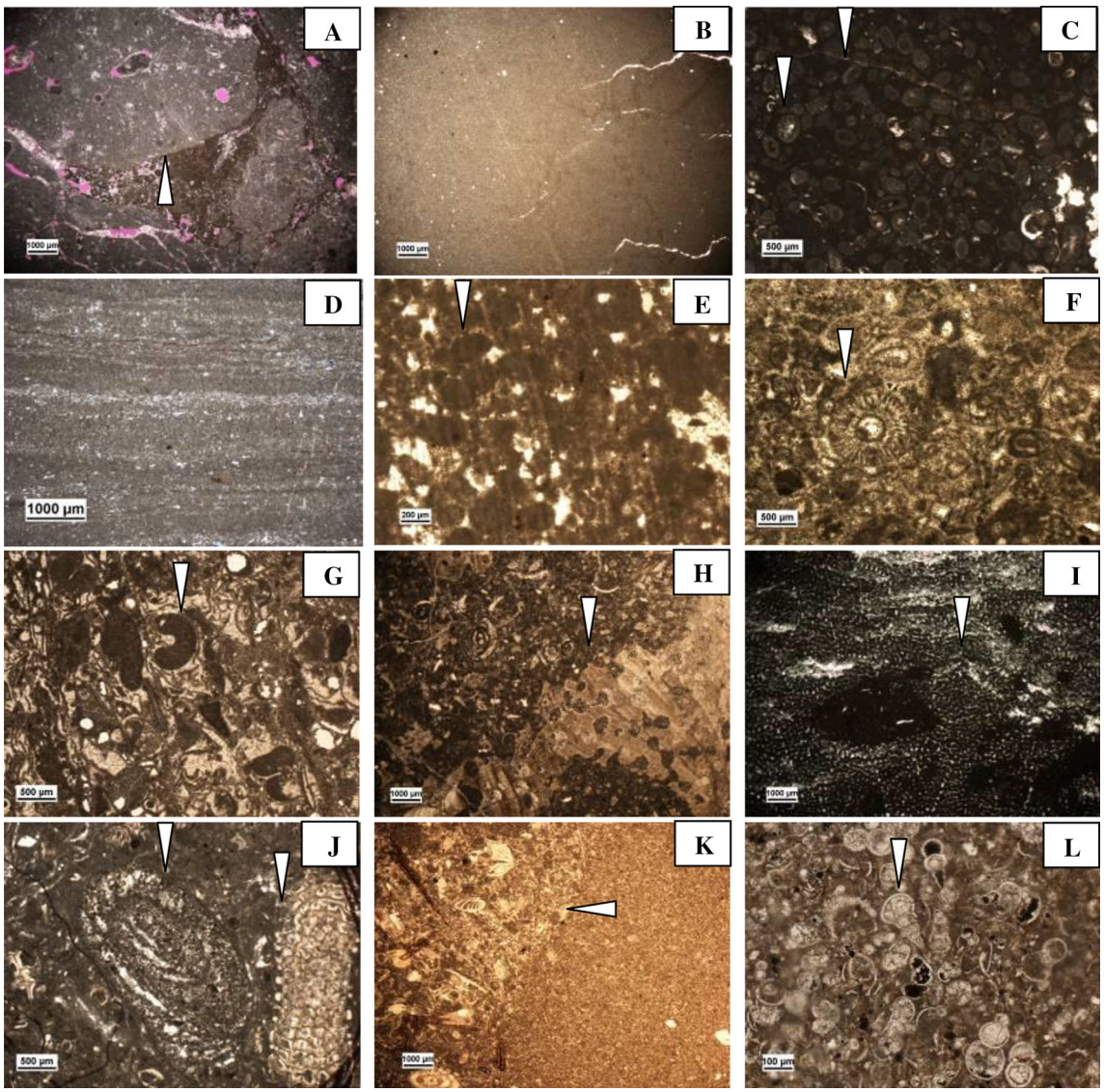

Fig. 4 Photomicrographs of different microfacies. **a** Intraclast rudstone (A1). XPL. **b** Dolomudstone (A2). PPL. **c** Ooid packstone (A3), PPL. **d** Stromatolite bindstone (A4), ppl. **e** Peloid packstone (B1). PPL. **f** Dacyclad bioclast packstone (B2) PPL. **g** Peloid bioclast packstone (C1), PPL. **h** Bioclast rudist debris floatstone (D1), PPL. **i** Coral bafflestone (D2), PPL. **j** *Omphalocyclus Loftusia* Packstone (E1), PPL. **k** Calciturbidite (E2), and PPL. **l** Planktonic foraminifera packstone (F1), PPL

equivalent to SMF 18 of Flügel (2010). The presence of miliolids shows a very shallow water environment, with subsaline-to-hypersaline conditions. They live preferably in low-turbulence water, where abundant sediment fines occur (Hottinger 1997, 2007; Geel 2000).

The presence of porcelaneous benthic foraminifera such as miliolids and textularids in a muddy background, low diversity of benthic foraminifera, and the presence of dacyclad green algae, pervasive dolomitization, and association with tidal flat microfacies in vertical interval indicate that B1 and B2 were deposited in the restricted lagoon (Flügel 2010). Green algae are abundant in the upper Cretaceous deposits of the Zagros successions and representing shallow warm water with relatively high salinity (Riding 1991; Mosadegh and Shirazi 2009; Mehrabi et al. 2015).

Open lagoon facies' belt

This group of facies is mainly packstone in texture dominated by benthic foraminifers such as *Cuneolina* sp., *Nezzazata* sp., *Minouxia* sp., *Dicyclina shlumbergeri, Rotalia* sp., *Valvulina* sp., *Sirtina* sp., *Coskinolina* sp., *Nezzazatinella* sp., *Dictioconous* sp., *Loftusia* sp, and *Omphalocyclus* sp. in combination with gastropods, ostracod, coral, rudist and dacyclad, as well as echinoderm and bivalve debris (Fig. 4g). Peloids (30–40%) are the main non-skeletal allochems of this microfacies. Micritization and

bioturbation are common. High diversity benthic foraminifera indicate the normal salinity of the sea water and abundant microfauna indicates prolific conditions (Purser 1973; Palma et al. 2007; Jamalian et al. 2010).

Reefal facies' belt

Reefal facies includes: D1-Rudistic facies which are organized in packstone, grainstone, floatstone, rudstone, and boundstone textures. Rudists are mainly radiolitidae and rarely hiporitidae types and their amount reach to 10–50%. In addition, lagoonal fauna such as *Cuneolina* sp., *Nezzazata* sp., *Minouxia* sp., *Dicyclina shlumbergeri*, Miliolide, *Valvulina* sp., *Sirtina* sp., *Coskinolina* sp., *Nezzazatinella* sp., and *Dictioconous* sp. are also present (Fig. 4h). Boring and neomorphism strongly affected the rudist shells. Internal sediment, micrite, and sparry calcite cement filled the internal pores of the rudists. This microfacies is equivalent to SMF 7 of Flügel (2010). D2-Coral bearing facies with bafflestone texture (Fig. 4i). The cavity of the corals filled with micrite or sparite. Benthic foraminifera and shell debris are subordinates. These microfacies were deposited in reef setting.

E-Open marine facies' belt

This group of facies can be divided into three kinds of microfacies: E1-Benthic foraminiferal dominated facies which are organized mostly in packstone texture. The bioclast components include *Omphalocyclus macroporous*, *Loftusia* sp., *Siderolites calcitrapoides*, *Orbitoides* sp. as well as rudist, echinoderm, and bivalve debris associated with non-skeletal grain like peloids (Fig. 4j). Omphalocyclcus are index fossils of Tethyan realm (Ozcan 2007) and lived in the upper part of photic zone and mostly observed in the upper part of shallowing upward cycles (Hottinger 1983; Moro et al. 2002; Abramovich and Keller 2002). E2-Calciturbidites consist of mixed planktonic and benthic foraminifers. This microfacies is characterized by the presence of large intraclasts in basinal microfacies (fine-grained bioclast packstone). Intraclasts contain bioclasts of shallower parts including bioclasts of *Siderolites calcitrapoides* and *Rotalia* sp. (Fig. 4k).

F-Basinal facies' belt

F1-Planktonic foraminiferal dominated facies containing *Globotruncana* sp., *Globigerina* sp., *Oligostegina* sp. (10%), sponge spicule (3%), *Radiolaria* sp., and echinoderm (15%) (Fig. 4l). This facies sometimes includes smaller planktonic foraminifera such as *Globotruncana* sp. and *Globotruncana stuarti* with pyritization in a muddy matrix. This microfacies is equivalent to SMF 1 of Flügel (2010).

Maastrichtian depositional environments

Six microfacies' belts have been identified based on the types and percentage of allochems, vertical change of microfacies, and correlation to the standard microfacies of Wilson (1975) and Flügel (2010). The presence of calciturbidites, lens form rudist patch reefs and rapid changes of microfacies, led us to consider a shelf carbonate platform with marginal rudist patch reefs for these deposits (Fig. 5). Accordingly, belts A, B, and C were deposited in the inner part of shelf, rudist patch reefs facies' belt D in the shelf margin, and facies' belts E and F in outer shelf and basinal environments, respectively.

In the studied transect, in the northern part (i.e. Kuh-e Chadur), inner shelf and shelf margin deposits are dominated deposits, while toward the south (Ku-e Parak), the outer shelf deposits are dominated. In the south most section of the studied transect (Bavush-1), only basinal facies (Gurpi Formation) are present.

Salt tectonic effects on the sedimentary system

Among the studied sections, the Kuh-e Gach section is located near a salt plug, and consequently, the Maastrichtian deposits (Tarbur Formation) were affected by the presence of salt plug. It influenced locally the accommodation spaces during the Maastrichtian (indicated by decreasing thickness of Maastrichtian deposits). This can be documented by variations in thickness, facies and types and intensity of the diagenetic processes. The most significant diagenetic processes affected the Maastrichtian strata on salt plug are as below:

Dolomitization: Dolomitization is the most important diagenetic process which has taken place related to the salt plug. Two forms of dolomite are present:

1. *Coarse xenotopic fabric-destructive dolomite (dolosparite)* (Fig. 6a). This type of dolomite has mainly occurred in the lower part of Tarbur Formation (in TST of Maas-3 sequence) close to the salt plug. Poikilotopic anhydrite cement was also formed around the xenotopic dolomite crystals (Fig. 6b). The nearby salt plug was the source of hypersaline brines that injected the soluble anhydrite to adjacent layers.
2. *Fine crystalline fabric-retentive dolomite* (Fig. 6c, d). Toward the upper part of interval, far from the source of dolomitizing fluid (salt plug), the supersaturation of dolomitizing fluid decreased. Consequently, finer crystals of dolomites mimically replaced both matrix and grains of the precursor limestone.

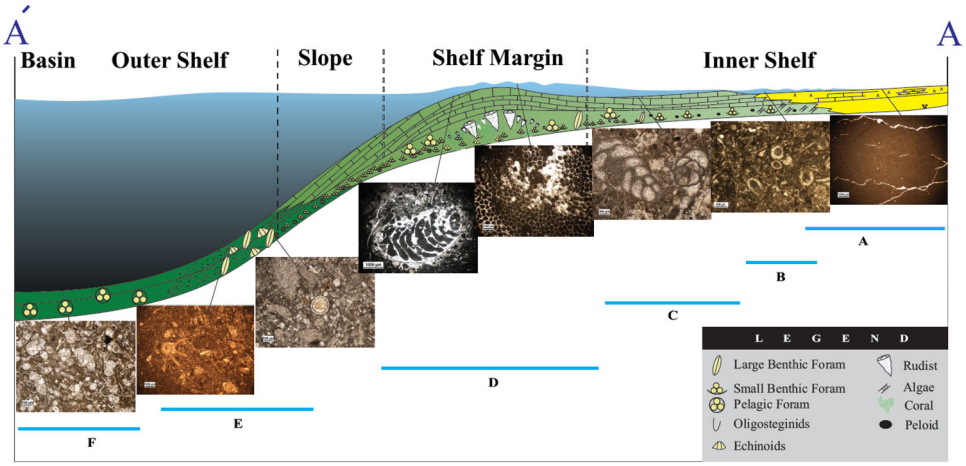

Fig. 5 Photomicrographs and relative position of facies belts shown in a schematic depositional model of the Maastrichtian sequences in the eastern part of Fars area

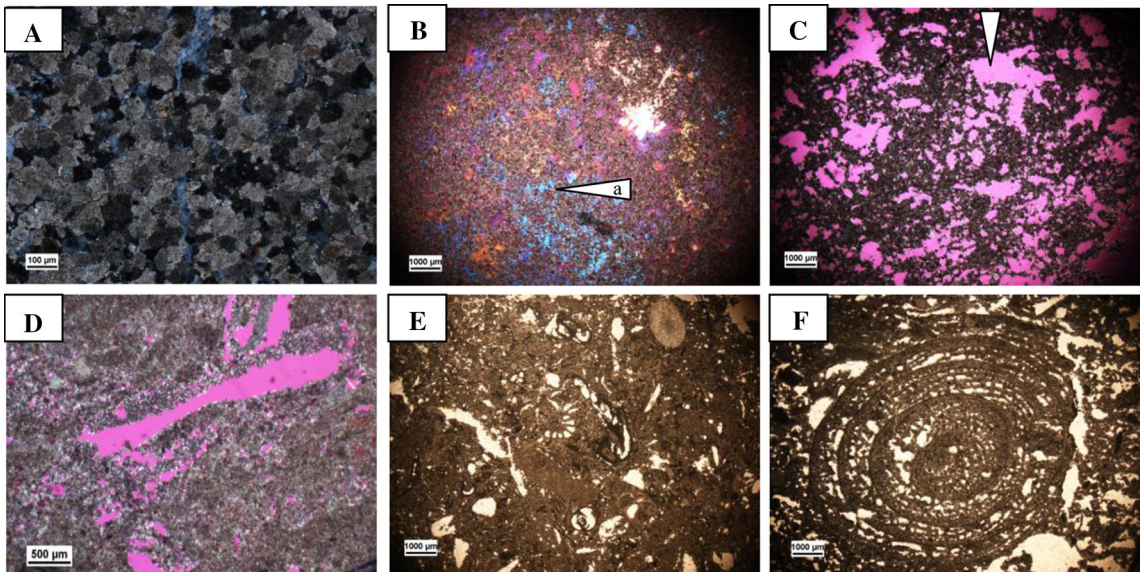

Fig. 6 Salt plug-related diagenetic features in the Maastrichtian deposits. Diagenetic processes in the zone 1, near salt plug. **a** Coarse xenotopic fabric-destructive dolomite crystals, XPL. **b** Poikilotopic anhydrite cement around xenotopic dolomite crystals, XPL. **c** Vuggy porosity in zone 2, XPL. **d** Moldic porosity after *Omphalocyclus macroporous*. Ghosts of allochems are also observed. XPL. Diagenetic processes in zone 3 (far from the salt plug). As the figures show, the effects of dolomitization decreased and dolomitization is fine crystalline and fabric-retentive. **e** Fine-crystalline dolomite with fabric-retentive texture. Diverse benthic foraminifera can be identified. PPL. **f** Fabric-retentive dolomitization of *Loftusia* sp. PPL

Dissolution: Dissolution is another diagenetic process occurred in the Maastrichtian deposits. Undersaturated fluids with respect to unstable to metastable minerals (e.g., aragonite and HMC) originated from salt plug have resulted in the formation of moldic (Fig. 6e) and vuggy porosity (Fig. 6f) (in Maas-3 sequence). In a similar trend, in comparison with the dolomitization, the intensity of dissolution has considerably decreased away from the salt plug. This confirms that the both dolomitizing and dissolving fluids were originated from the salt plug (Fig. 7).

Accordingly, a generally zonation was identified around the salt plug (Fig. 7).

Zone-1 This zone presents in adjacent to the salt plug that consists of coarse xenotopic fabric-destructive dolomite crystals along with anhydrite cement. This zone presented in the lower part of Tarbur Formation.

Zone-2 It is the transitional zone between 1 and 3. Ghosts of allochems and intense dissolution can be observed.

Zone-3 This zone is far from salt plug and consists of fine crystalline fabric-retentive dolomitization and allochems are well-preserved. This zone presented in the uppermost part of the Tarbur Formation.

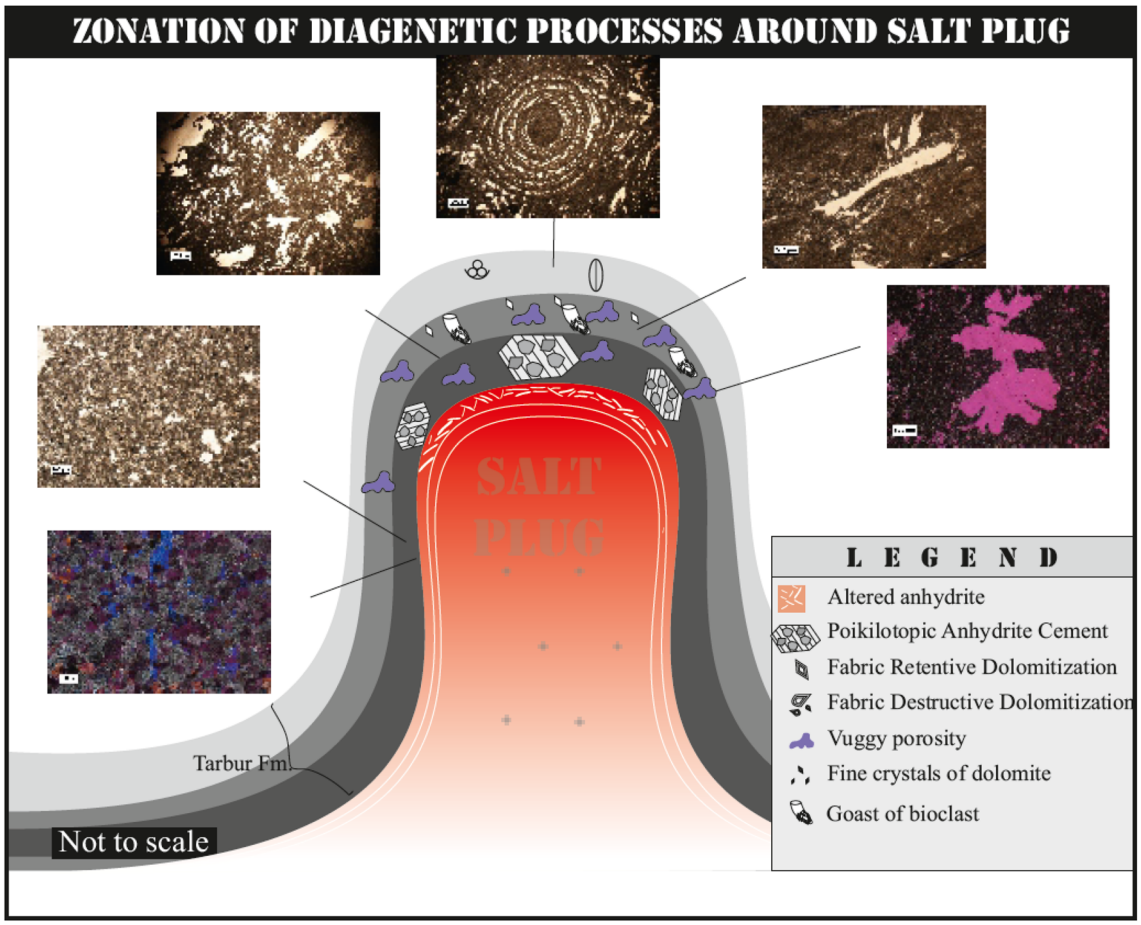

Fig. 7 Diagenetic processes around the salt plug. As the figure shows, there is zonation around the salt plug. Zone 1-Near salt plug, coarse xenotopic fabric-destructive dolomitization along with anhydrite cement are present. Toward the upper part of the interval, zone-2 with ghosts of allochems and intense dissolution; zone-3 with fine crystalline fabric-retentive dolomitization can be observed

Sequence stratigraphy

To stepping the tectono-sedimentary events through the Maastrichtian, a sequence stratigraphic approach has been used to explain the distribution of depositional facies, diagenetic features, thickness variation, and bedding pattern in the both local and regional scales through the time and space. In terms of dating, age of the Maastrichtian is based either on the presence of fore-reef assemblage zone in the shallow-water carbonate (Tarbur Formation) or on the presence of *Globotruncana stuarti–Pseudotextularia varians* assemblage zone [zone 37 of Wynd (1965)] in the basinal setting (Gurpi Formation). This dating is not precise enough for the high-resolution sequence stratigraphy in the Maastrichtian scale. In addition, many parts of the sections are barren and Maastrichtian interval cannot be easily defined. Therefore, the prepared sequence stratigraphic framework is mainly based on regional correlation. On the other hand, effects of salt plugs on the sedimentary system have resulted in intensive diagenetic influences and reducing dating resolution. In this case, recognizing some key levels on the gamma ray logs can be helpful to establish a sequence stratigraphic framework. Accordingly, five 4th-order sedimentary sequences have been defined through the Maastrichtian interval and their variation studied along a regional NE–SW trending transect (Figs. 8, 9 and 10). Plaeogeographic maps are also prepared for each sequence to reconstruct the sequence stratigraphic-based depositional history of the Maastrichtian sequences in the eastern Fars area (Fig. 11).

Sequence Maas-1

This sequence is observed only in northern part of the basin (Kuh-e Chadur; see Fig. 1 for location) and dies out toward the south. The lower sequence boundary lies above the radiolarites can be considered as a type-I sequence boundary. Transgressive systems tract (TST) deposits of this sequence are not totally recorded in Kuh-e Chadur section. Highstand systems tract (HST) consists of *Loftusia Omphalocyclus* packstone (E1) of the proximal open marine environment. It changes upward to massive layer of

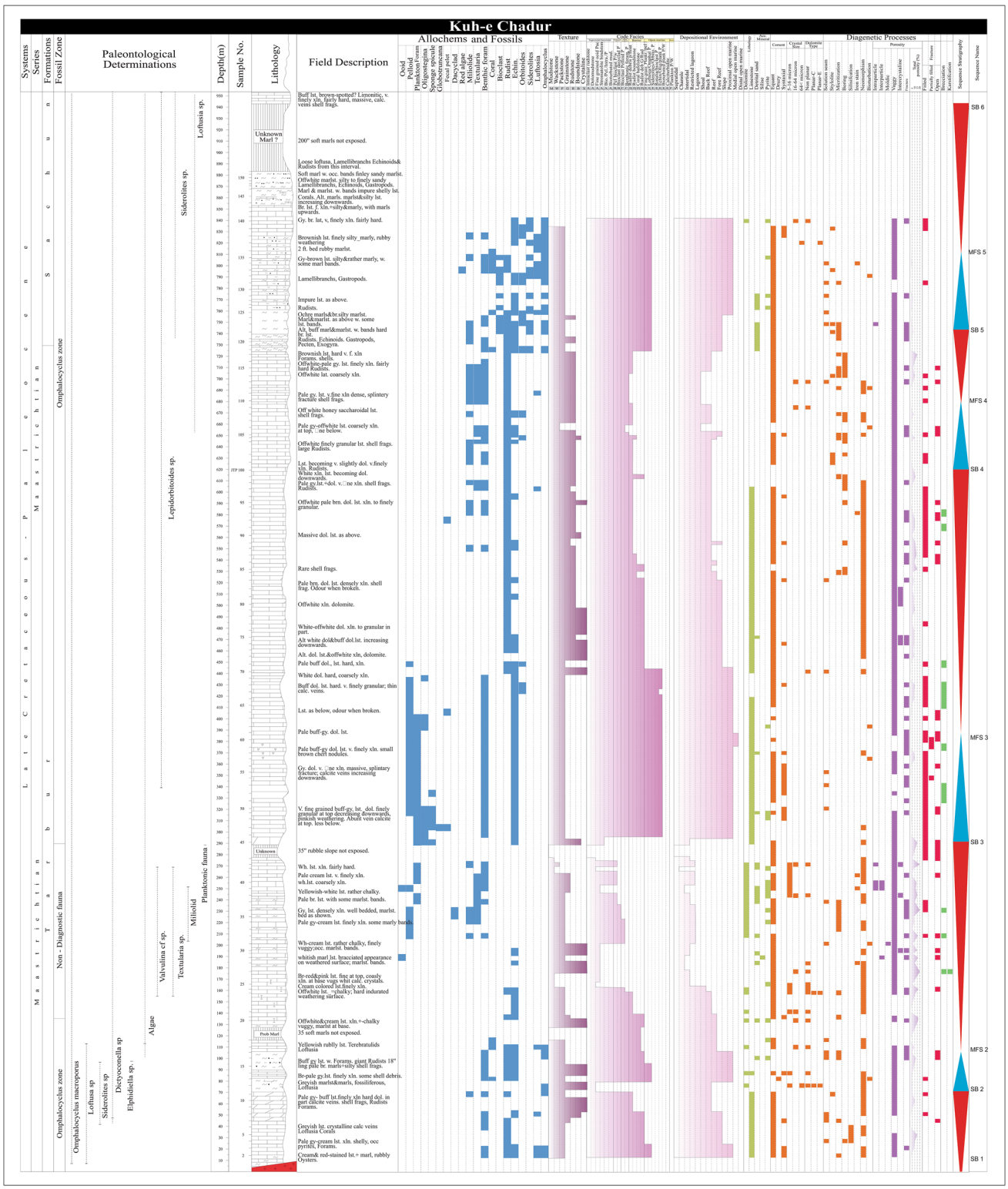

Fig. 8 Petrographical and sedimentological logs of the Maastrichtian deposit in Kuh-e Chadur

rudist debris packstone to floatstone of the fore reef (talus) and followed by coral bafflestone (D2) and bioclast packstone of back-reef lagoonal environment. The upper boundary (SB1) is marked by dissolution (Fig. 12a), dolomite recrystallization (Fig. 12b), neomorphism, meteoric calcite cementation, and Fe-staining. This sequence

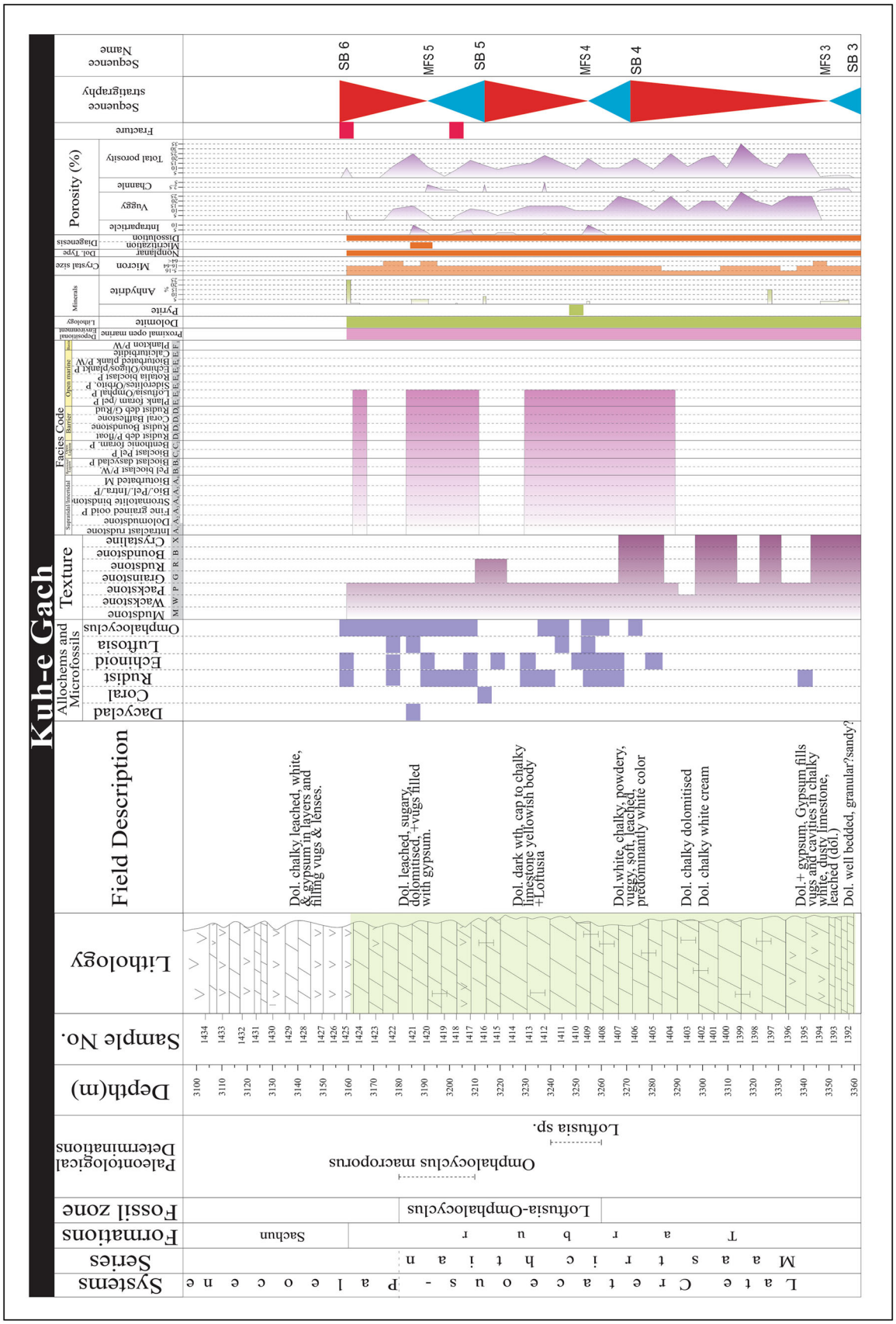

Fig. 9 Petrographical and sedimentological logs of the Maastrichtian deposit in Kuh-e Gach section

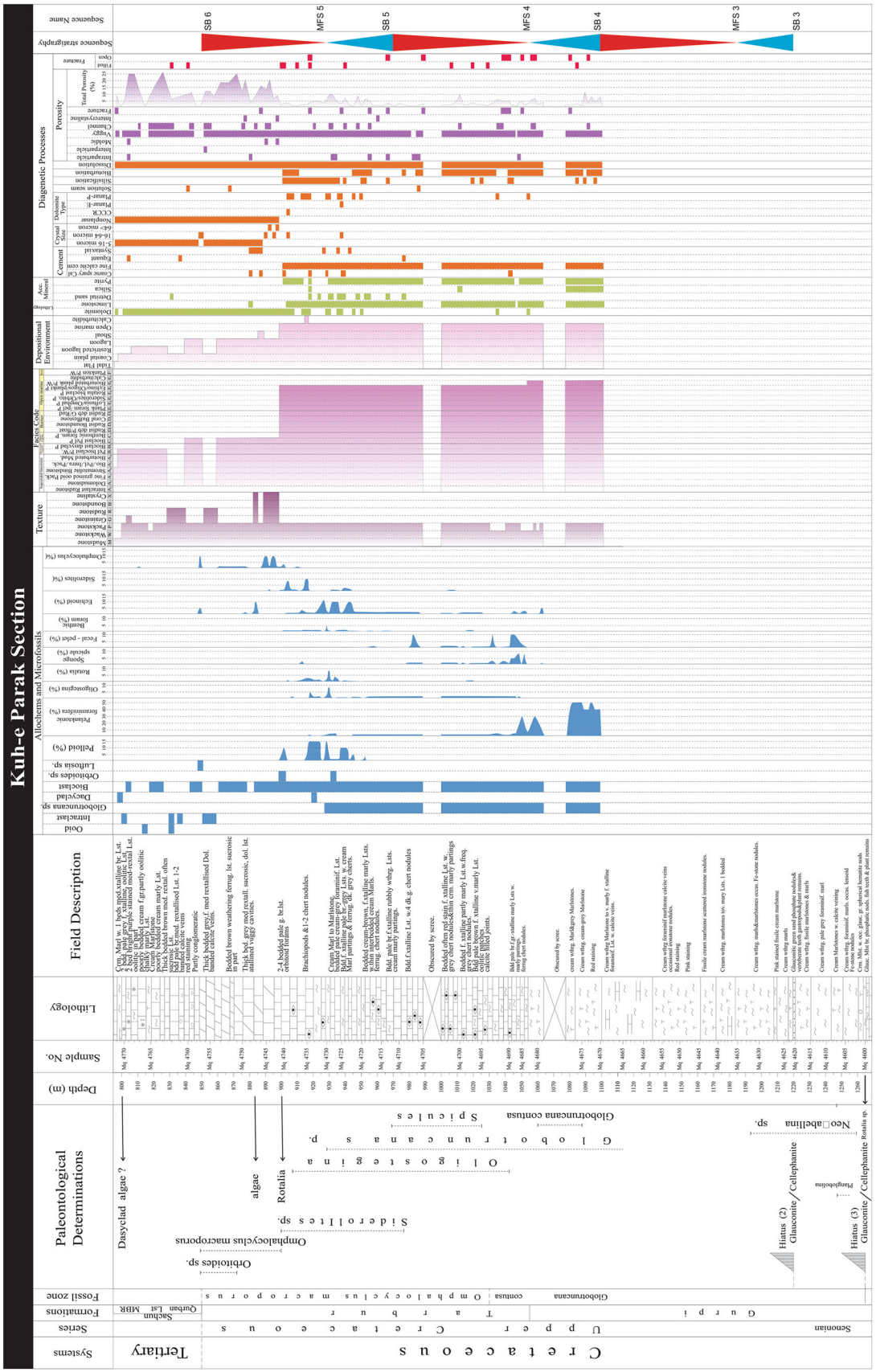

Fig. 10 Petrographical and sedimentological logs of the Maastrichtian deposit in Kuh-e Parak section

downlapped toward the south and did not present in the southern sections, such as Kuh-e Gach and Parak. The thickness of this sequence is about 70 m.

Paleogeographic map (Fig. 11a) of this sequence shows that a carbonate platform was present in the northeast of the basin. Rudist patch reefs in association with corals were formed in this area.

Sequence Maas-2

This sequence is observed only in the northern part (i.e. Chadur section). The lower boundary of this sequence in northern part (Kuh-e Chadur section) is SB1. The thickness of this sequence is about 220 m. The TST consists of intercalation of marl and limestone with *Omphalocyclus* bioclast packstone of proximal open marine environment. Top of the marly unit (in 105 m) considered as MFS. The HST is composed of rudist debris packstone to floatstone, coral bafflestone, and bioclast floatstone of fore-reef (talus) depositional setting. They change upward to lagoon and tidal flat microfacies (A4 and A3). The upper boundary (SB3) has evidence of karstic features (Fig. 12c) such as calcite cements (Fig. 12d), recrystallization, brecciation, and Fe-staining (Fig. 12e) and pink to red color in the field view was identified as SB1.

Based on paleogeographic map (Fig. 11b, c), it can be concluded that a carbonate platform with rudist patch reef in its inner parts was dominated the study area, during deposition of this sequence. Depocenter of this sequence was located in the northern part, in the Chadur section.

Sequence Maas-3

The upper (SB4) and lower (SB3) boundaries of this sequence are type 1 in northern part of the basin (Kuh-e Chadur section). Intense dissolution and high amount of vuggy porosity, Fe-staining, dolomitization, neomorphism, and brecciation (Fig. 12g) are evidence of exposure. Toward the south, both of them grades to type-II sequence boundary. This is as a result of the formation in the foreland basin. Northern section (Kuh-e Chadur section) is located on the forebulge, while toward the south the other sections formed in the backbulge of the foreland basin. TST (in Kuh-e Chadur section) consists of fine-grained peloid bioclast echinoderm packstone of proximal open marine environment. Toward the south (Kuh-e Parak section), it grades to the pelagic marl of Gurpi Formation and consists of fine-grained bioclast planktonic foraminifera packstone of basinal environment with *Globigerina sp.*, *Globotruncana* sp., sponge spicule, and other planktonic foraminifera.

In Pishvar-1 well, TST is composed of *Oligostegina sp.*, *Heterohelix* sp., *Pithonella* sp., *Hedbergella* sp., spicule sponge and calcispherula. Maximum flooding surface includes the deepest facies characterized by the high GR log response. In HST, echinoderm, bryozoa debris, and benthic foraminifera can be observed.

Fig. 11 Palaeogeographic evolution of study area during Maas-1 to Maas-5 sequences for TST and HST systems tracts. For preparing these maps, the data of the adjacent area were also used. These maps show foreland basin migration from northwest toward southeast ▶

Maximum flooding surface (MFS-3) is identified by the presence of *Oligostegina* sp. in E1 microfacies (in Kuh-e Chadur) which shows the most deepening and shows the highest values of GR on well logs (Pishvar-1). This surface can be correlated with the K180 of Sharland et al. (2001) in other parts of the Arabian Plate (Fig. 13).

HST consists of rudist zone with D1 and D2 microfacies of fore reef, reef, and back reef, respectively, in northern part (Kuh-e Chadur). Toward the southern part (Kuh-Parak), it grades to outer shelf environment and includes sponge spicule, echinoderm, *Rotalia*, planktonic foraminifera, and fecal pellets.

In Kuh-e Gach section around the salt plug, this sequence was also completely dolomitized. In TST, the ghost of rudist debris along with *Loftusia* sp., *Omphalocyclus* sp., echinoderm, and algae can be observed which are the evidence of deposition in the paleaohigh with a small rudist zone. HST consists of *Loftusia*, benthic foraminifera, rudist debris, echinoderm, and algae of inner shelf.

In general, the facies is prograded from NE to SW. In northeast, the TST consists of rudist zone of mid shelf which is grades to outer shelf deposits in Kuh-e Parak section and basinal deposits (Gurpi Formation). In northern part, the HST consists of inner/mid shelf deposits, which grades to outer shelf deposits in Kuh-e Parak and Pishvar-1 sections. Maximum flooding surface includes the deepest facies characterized by the high GR log response in subsurface section (Pishvar-1) and marly unit in surface section (Kuh-e Chadur).

Paleaogeographic map of this sequence is present in Fig. 11d, e. As these maps indicate, a carbonate platform with shelf marginal rudist patch reefs is present in the northern parts. Toward the south and southeast, outer shelf and basinal depositional setting are present.

Sequence Maas-4

The upper boundary (SB5) is type-II in Chadur section and identified by facies' changes form lagoon/back reef to proximal open marine environment. In this section, the TST consists of rudist reef facies which progrades toward the south to basinal *Globotruncana* marl of the Gurpi Formation in Kuh-e Parak section. HST consists of inner

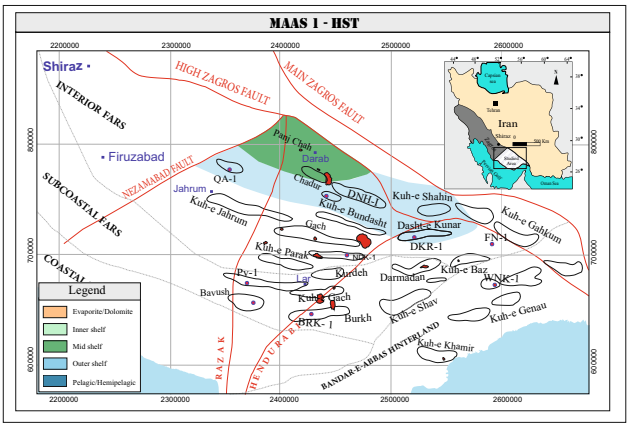
MAAS 1 - HST
Shiraz
Firuzabad
INTERIOR FARS
SUBCOASTAL FARS
COASTAL
HIGH ZAGROS FAULT
MAIN ZAGROS FAULT
NEZAMABAD FAULT
Panj Chah
Darab
Chadir
QA-1
Jahrum
Kuh-e Jahrum
DNH-1
Kuh-e Bundasht
Gach
Kuh-e Shahin
Dasht-e Kunar
DKR-1
FN-1
Kuh-e Gahkum
Kuh-e Parak
NPK-1
Py-1
Lar
Kurdeh
Darmadan
Kuh-e Baz
WNK-1
Bavush
Kuh-e Gach
BRK- 1
Burkh
Kuh-e Shav
Kuh-e Genau
Kuh-e Khamir
RAZAK
HENDURABI
BANDAR-E-ABBAS HINTERLAND
Iran
Legend
Evaporite/Dolomite
Inner shelf
Mid shelf
Outer shelf
Pelagic/Hemipelagic

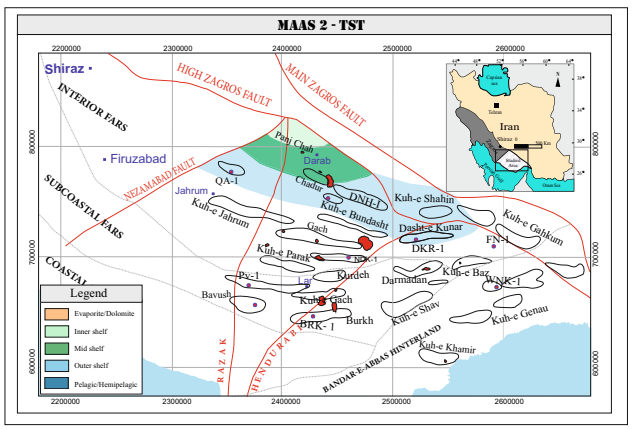
MAAS 2 - TST
Shiraz
Firuzabad
INTERIOR FARS
SUBCOASTAL FARS
COASTAL
HIGH ZAGROS FAULT
MAIN ZAGROS FAULT
NEZAMABAD FAULT
Panj Chah
Darab
Chadir
QA-1
Jahrum
Kuh-e Jahrum
DNH-1
Kuh-e Bundasht
Gach
Kuh-e Shahin
Dasht-e Kunar
DKR-1
FN-1
Kuh-e Gahkum
Kuh-e Parak
NPK-1
Py-1
Lar
Kurdeh
Darmadan
Kuh-e Baz
WNK-1
Bavush
Kuh-e Gach
BRK- 1
Burkh
Kuh-e Shav
Kuh-e Genau
Kuh-e Khamir
RAZAK
HENDURABI
BANDAR-E-ABBAS HINTERLAND
Iran
Legend
Evaporite/Dolomite
Inner shelf
Mid shelf
Outer shelf
Pelagic/Hemipelagic

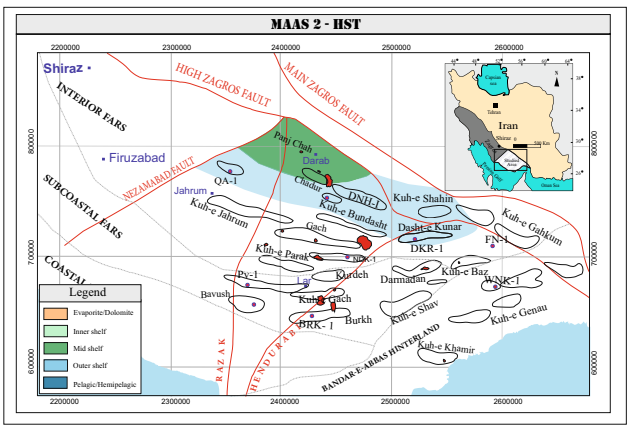
MAAS 2 - HST
Shiraz
Firuzabad
INTERIOR FARS
SUBCOASTAL FARS
COASTAL
HIGH ZAGROS FAULT
MAIN ZAGROS FAULT
NEZAMABAD FAULT
Panj Chah
Darab
Chadir
QA-1
Jahrum
Kuh-e Jahrum
DNH-1
Kuh-e Bundasht
Gach
Kuh-e Shahin
Dasht-e Kunar
DKR-1
FN-1
Kuh-e Gahkum
Kuh-e Parak
NPK-1
Py-1
Lar
Kurdeh
Darmadan
Kuh-e Baz
WNK-1
Bavush
Kuh-e Gach
BRK- 1
Burkh
Kuh-e Shav
Kuh-e Genau
Kuh-e Khamir
RAZAK
HENDURABI
BANDAR-E-ABBAS HINTERLAND
Iran
Legend
Evaporite/Dolomite
Inner shelf
Mid shelf
Outer shelf
Pelagic/Hemipelagic

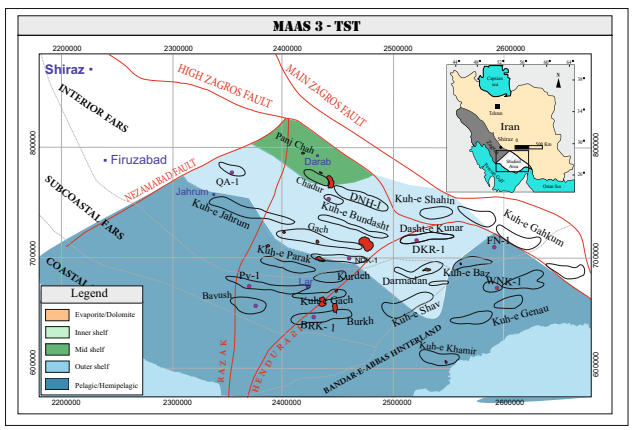
MAAS 3 - TST
Shiraz
Firuzabad
INTERIOR FARS
SUBCOASTAL FARS
COASTAL
HIGH ZAGROS FAULT
MAIN ZAGROS FAULT
NEZAMABAD FAULT
Panj Chah
Darab
Chadir
QA-1
Jahrum
Kuh-e Jahrum
DNH-1
Kuh-e Bundasht
Gach
Kuh-e Shahin
Dasht-e Kunar
DKR-1
FN-1
Kuh-e Gahkum
Kuh-e Parak
NPK-1
Py-1
Lar
Kurdeh
Darmadan
Kuh-e Baz
WNK-1
Bavush
Kuh-e Gach
BRK- 1
Burkh
Kuh-e Shav
Kuh-e Genau
Kuh-e Khamir
RAZAK
HENDURABI
BANDAR-E-ABBAS HINTERLAND
Iran
Legend
Evaporite/Dolomite
Inner shelf
Mid shelf
Outer shelf
Pelagic/Hemipelagic

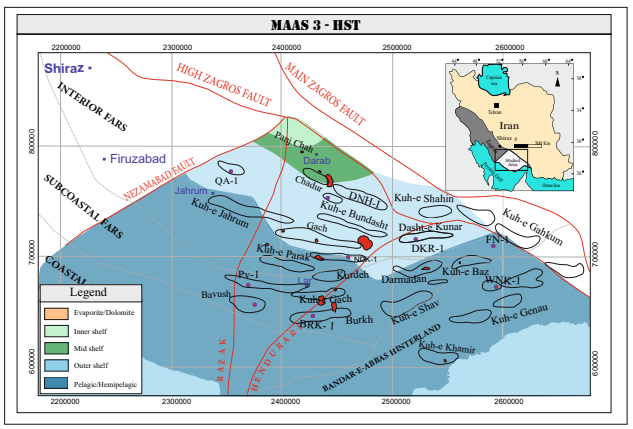
MAAS 3 - HST
Shiraz
Firuzabad
INTERIOR FARS
SUBCOASTAL FARS
COASTAL
HIGH ZAGROS FAULT
MAIN ZAGROS FAULT
NEZAMABAD FAULT
Panj Chah
Darab
Chadir
QA-1
Jahrum
Kuh-e Jahrum
DNH-1
Kuh-e Bundasht
Gach
Kuh-e Shahin
Dasht-e Kunar
DKR-1
FN-1
Kuh-e Gahkum
Kuh-e Parak
NPK-1
Py-1
Lar
Kurdeh
Darmadan
Kuh-e Baz
WNK-1
Bavush
Kuh-e Gach
BRK- 1
Burkh
Kuh-e Shav
Kuh-e Genau
Kuh-e Khamir
RAZAK
HENDURABI
BANDAR-E-ABBAS HINTERLAND
Iran
Legend
Evaporite/Dolomite
Inner shelf
Mid shelf
Outer shelf
Pelagic/Hemipelagic

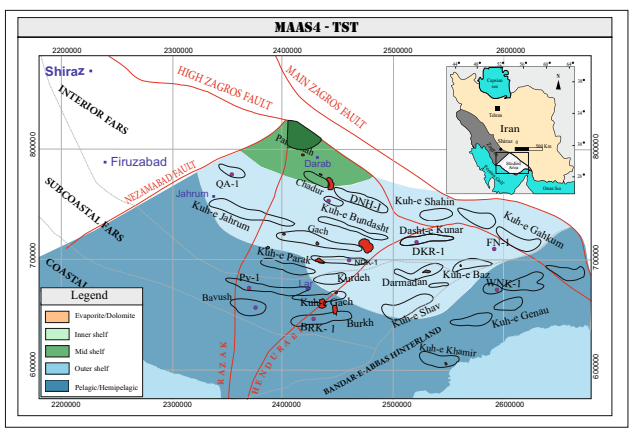
MAAS4 - TST
Shiraz
Firuzabad
INTERIOR FARS
SUBCOASTAL FARS
COASTAL
HIGH ZAGROS FAULT
MAIN ZAGROS FAULT
NEZAMABAD FAULT
Panj Chah
Darab
Chadir
QA-1
Jahrum
Kuh-e Jahrum
DNH-1
Kuh-e Bundasht
Gach
Kuh-e Shahin
Dasht-e Kunar
DKR-1
FN-1
Kuh-e Gahkum
Kuh-e Parak
NPK-1
Py-1
Lar
Kurdeh
Darmadan
Kuh-e Baz
WNK-1
Bavush
Kuh-e Gach
BRK- 1
Burkh
Kuh-e Shav
Kuh-e Genau
Kuh-e Khamir
RAZAK
HENDURABI
BANDAR-E-ABBAS HINTERLAND
Iran
Legend
Evaporite/Dolomite
Inner shelf
Mid shelf
Outer shelf
Pelagic/Hemipelagic

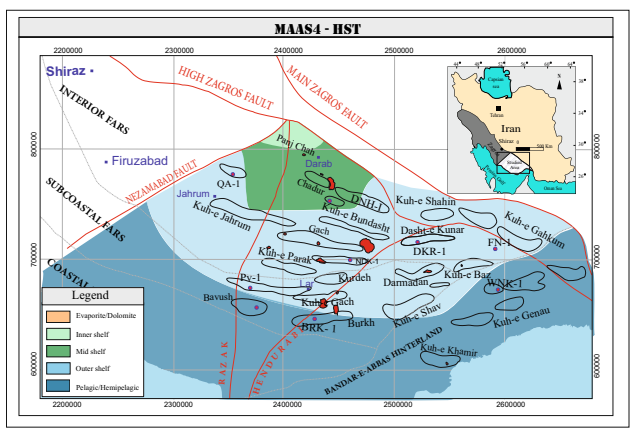
MAAS4 - HST
Shiraz
Firuzabad
INTERIOR FARS
SUBCOASTAL FARS
COASTAL
HIGH ZAGROS FAULT
MAIN ZAGROS FAULT
NEZAMABAD FAULT
Panj Chah
Darab
Chadir
QA-1
Jahrum
Kuh-e Jahrum
DNH-1
Kuh-e Bundasht
Gach
Kuh-e Shahin
Dasht-e Kunar
DKR-1
FN-1
Kuh-e Gahkum
Kuh-e Parak
NPK-1
Py-1
Lar
Kurdeh
Darmadan
Kuh-e Baz
WNK-1
Bavush
Kuh-e Gach
BRK- 1
Burkh
Kuh-e Shav
Kuh-e Genau
Kuh-e Khamir
RAZAK
HENDURABI
BANDAR-E-ABBAS HINTERLAND
Iran
Legend
Evaporite/Dolomite
Inner shelf
Mid shelf
Outer shelf
Pelagic/Hemipelagic

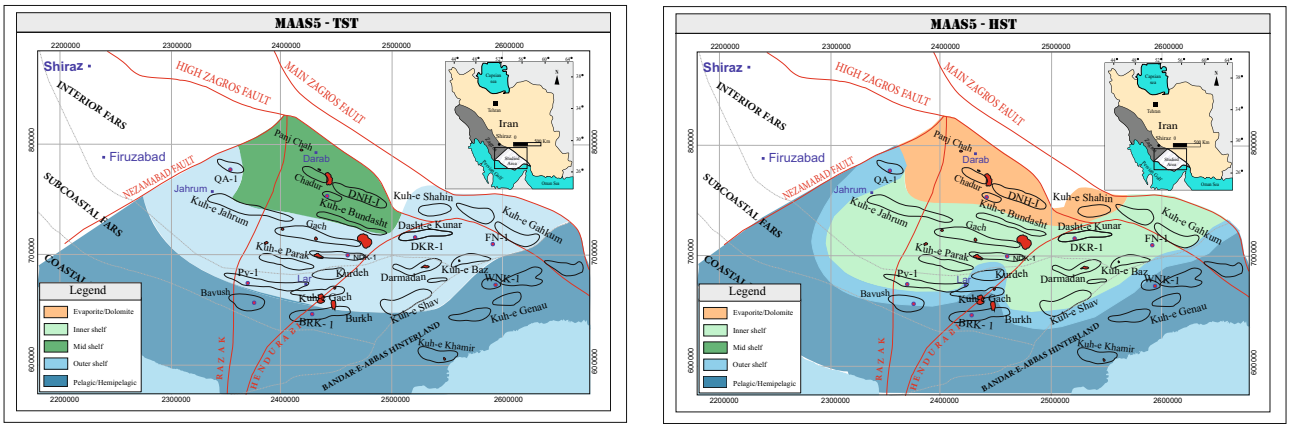

Fig. 11 continued

shelf deposits including lagoon to back-reef setting in the northern part. Toward the south, it grades to outer shelf deposits. The lower boundary (SB4) is type-I in Kuh-e Chadur section and type-II toward the south. Palaeogeographic maps of this sequence are presented in Fig. 11f, g. As the figures shown in Kuh-e Chadur section, rudist patch reefs are present in the north and progrades to basin toward the south.

Sequence Maas-5

In the northern part (Kuh-e Chadur), this sequence covers the lower part of Sachun Formation. The lower boundary is placed at top of the Tarbur Formation. The upper boundary is bounded by a regional unconformity (SB6) which is present throughout the Zagros and Arabian Plate (Sharland et al. 2001) (see Fig. 8). In Kuh-e Parak and Gach sections, intense dissolution, dolomitization (Fig. 12h), meteoric calcite cementation (Fig. 9d, i), dedolomitization (Fig. 12e), brecciation, Fe-staining (Fig. 12g) and neomorphism (Fig. 12i) are the evidence of exposure during K/T unconformity. K/T unconformity is an important boundary in geological history that marks with planktonic bioevents (Farouk 2014), faunal change, benthic foraminiferal diversity and assemblages changes (Farouk and Jain 2016) or mass extinction (Keller 2012). In the studied sections, most of fuana such as *Loftusia* sp., *Siderolites* sp. *Omphalocyclus* sp., and *Orbitoides* sp. were extinct.

In Kuh-e Chadur, the TST consists of intercalation of marl and marly limestone with *Siderolites* sp., *Loftusia* sp. echinoid and lamelibranch which was deposited in the outer shelf environment. Toward the south, this sequence grades to top of the Tarbur Formation. Lithology of TST (Kuh-e Parak) is limestone with fine-grained *oligostegina* echinoderm bioclast packstone (F1). Sponge spicule, *Rotalia* sp. and *Siderolites* sp. are also present as subordinate grains. This systems tract was deposited in outer to mid shelf environment.

In Pishvar-1 section, the upper and lower boundaries are distinguished by high GR values. In this section, the TST consists of echinoid, *Oligostegina* sp., and planktonic foraminifera and *Cibicides* sp. of outer shelf.

The lower boundary in northern part is a type-I sequence boundary that characterized by Fe-staining, neomorphism and dissolution. Toward the south, it grades to a type-II boundary. In Pishvar-1, the lower boundary is distinguished by high GR values.

In northern part of the basin (Kuh-e Chadur), maximum flooding surface (MF-4) is located at top of a marly unit (in 974 m). In this section, the HST starts with carbonate layer and followed by dolomite and marly limestone. This part has poor fauna and only Valvulinds and Textularids are present. This systems tract was deposited in inner shelf environment in restricted lagoon. It finally ends with anhydrite layer of Cretaceous–Tertiary boundary.

In Kuh-e Parak section, HST consists of thick-bedded dolomite with skeletal *Omphalocyclus* packstone of lagoonal environment. Omphalocyclus are iron-stained and matrix is replaced by xenotopic dolomite. In Pishvar-1, HST consists of algae, shell fragments, and benthic foraminifera.

In general, from northeast toward the southwest thickness of this sequence decreased dramatically and in Bavush-1, this sequence is not recorded. There is an anomaly in thickness in Kuh-e Gach which is the result of salt plug. As shown in Figs. 10 and 12, the thickness of Maastrichtian deposits decreases dramatically in Kuh-e Gach section. Depositional environment is changed from

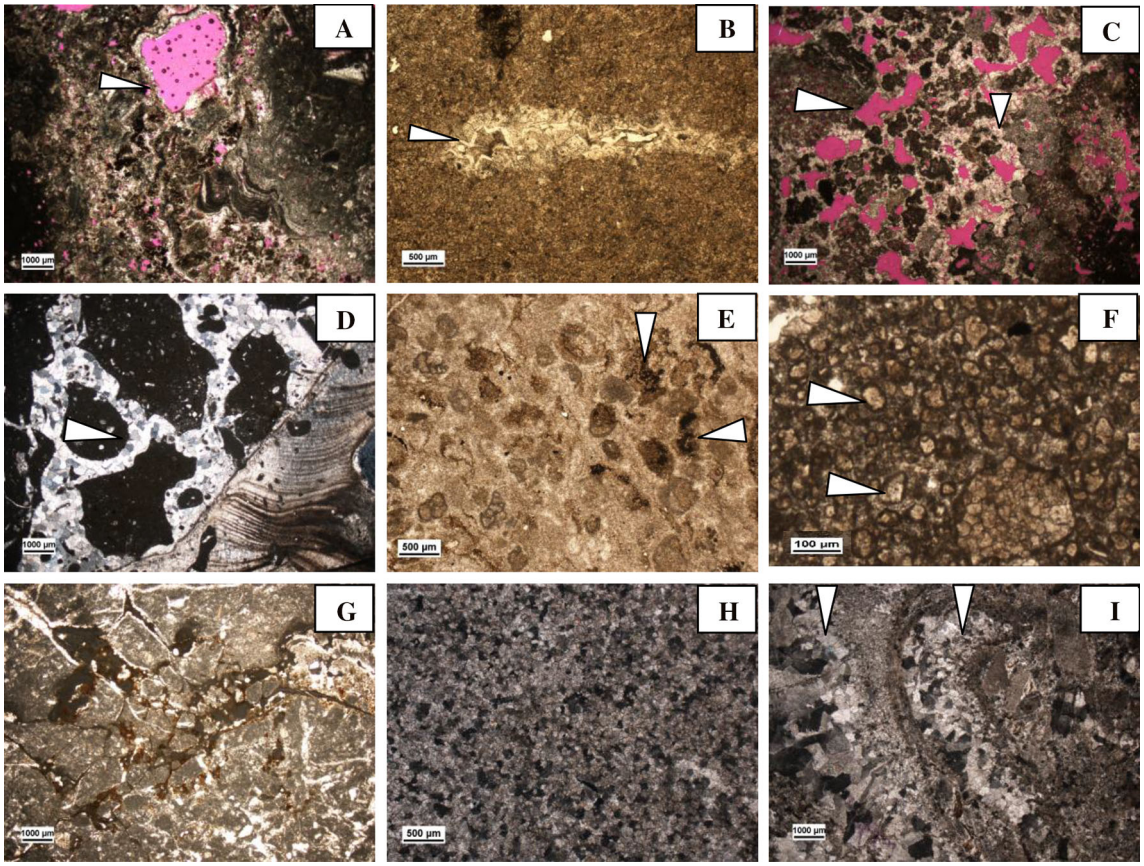

Fig. 12 Photomicrographs of distinct diagenetic processes identified in the sequence boundaries. **a** Dissolution forming isolated vugs. XPL. **b** Dolomitization. XPL. **c** Connected vugs as a result of intense dissolution. XPL. **d** Meteoric spary calcite cement. **e** Fe-staining of the allochems and matrix. XPL. **f** Dedolomitization, PPL. **g**. Brecciation along with Fe-staining, PPL. **h** Dolomitization. XPL. **i** Neomorphism in bioclast debris, XPL

inner shelf in north to outer shelf in the south and the facies progradationally migrate toward south. Palaeogeographic map of this sequence is presented in Fig. 11h, i.

Tectono-sedimentary evolution

To study tectono-sedimentary evolution of the Maastrichtian sequences, a perpendicular transect to the Zagros trend is selected (Fig. 14). In Kuh-e Chadur, north of the basin, Maastrichtian deposits are thick (1140 m) and include all five sequences. The sequences mostly consist of inner/mid shelf microfacies with rudist zone and proximal open marine environment. Depocenter of the basin was located in the northern part (Kuh-e Chadur). The presence of obducted radiolarites caused over thickening of the crust (Miall 2000) and additionally caused subsequent subsidence in the northern part of the basin (Kuh-e Chadur section). Toward the south (Kuh-e Parak, Pishvar-1 and Bavush-1), the thickness of sequences has decreased gradually. Based on the previous studies, the Maastrichtian deposits were deposited in a foreland basin (Piryaei et al. 2010, 2011). Therefore, the accommodation space decreased.

Based on high-resolution sequence stratigraphy performed along this transect, sequence Maas-1 and Maas-2 present only in northern part of the basin (i.e., Kuh-e Chadur).

Sequence Maas-3 presents in most of the sections. Depocenter in Sequence Maas-3 was located in northeastern part (i.e., Kuh-e Chadur) and the thickness decreased toward the SW. The dominate facies in n northeastern part (i.e. Kuh-e Chadur) are proximal open marine and rudist reefs in this sequence. These facies belt progrades toward the SW and change to basinal facies.

Sequence Maas-4 consists of rudist reef in northeastern part of the basin (i.e. Kuh-e Chadur) which progrades toward the SW to basinal *Globotruncana* marls of the Gurpi Formation in Kuh-e Parak section. The HST of this

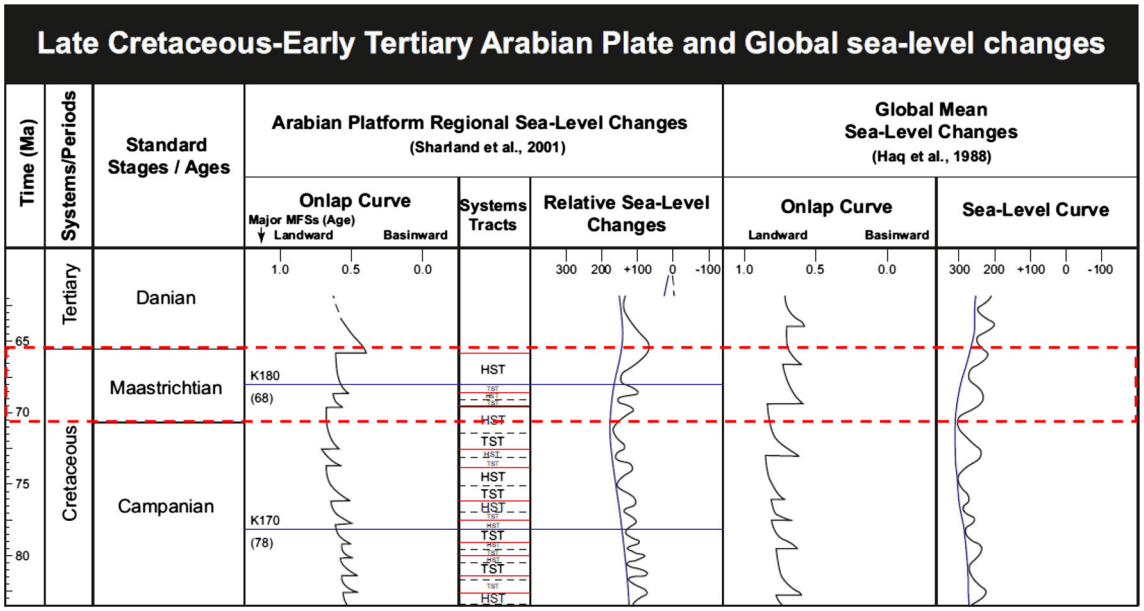

Fig. 13 Late Cretaceous–Early Maastrichtian Global and regional (Arabian Plate) mean sea-level changes (Haq et al. 1988; Sharland et al. 2001)

sequence in northeastern part (i.e., Kuh-e Chadur) consists of inner shelf deposits including lagoon to back-reef setting in the northern part, while toward the south, it grades to outer shelf deposits.

Sequence Maas-5 in northeastern part (i.e., Kuh-e Chadur) consists of dolomites and evaporites (restricted lagoon) of the (Sachun Formation) and grades to inner shelf deposits (lagoonal deposits) toward the south. In addition, the sequence thickness has also decreased form NE to SW.

Based on facies and thickness variations (Fig. 16), it can be concluded that Maastrichtian deposits are formed in a foreland basin. Carbonate deposits of Tarbur Formation are formed in bulge/forebulge setting and basinal facies of Gurpi Formation formed in back-bulge setting. Migration of depositional environments (Fig. 15), during different phases indicates bulge migration through different phases, which documented by sequence stratigraphic analysis. Based on this data, a schematic tectono-sedimentary model is prepared for Maastrichtian deposits in the eastern part of Fars area (Fig. 16).

Conclusions

To reconstruct tectono-sedimentary setting of the Maastrichtian deposits, five sections were selected perpendicular to the Zagros trend (NE–SW) in eastern part of the Fars area. As this transect revealed, thickness of Maastrichtian deposits decreased from NE toward SW. Facies' variations also show that progradation of microfacies has been occurred from NE toward SW. For example, sequence 3 in NE mainly consists of rudist reef facies which is grade to basinal deposits of Gurpi Formation toward the SW. Sequence 4 is also consists of rudist reefs of mid-shelf deposits in TST which progrades over the basinal facies of Gurpi Formation toward the south. In highstand systems tract, it consists of inner shelf deposits in NE and grades to outer shelf deposits with Oligosteginids, sponge spicule, echinoderm, and *Siderolites* sp. toward southwest.

In Sequence Maas-5 in NE, HST deposits consist of dolomites and evaporites of restricted lagoonal setting (Sachun Formation) which progrades to outer shelf to inner shelf deposits (in Parak section).

Based on thickness and facies' variation and depocenter migration, it can be concluded that Maastrichtian deposits in Fars area have been deposited in a foreland basin. In this basin, carbonates of Tarbur Formation have been deposited in forebulge/bulge, while basinal *Globotruncana* marls of the Gurpi Formation was formed in backbulge setting. Depositional model and paleogeographic maps during five sequences revealed that the depocenter migrates during the time.

In addition, salt tectonics was locally affected the Maastrichtian deposits. Salt tectonics caused formation of a paleohigh along the studied transect. It has resulted into decrease accommodation space and so sediment thickness decreased (e.g., in Kuh-e Gach section). Moreover, salt plug also caused different diagenetic effects including intense dolomitization, dissolution, and formation of anhydrite cements, mainly within the adjacent sediments. Types and intensity of such

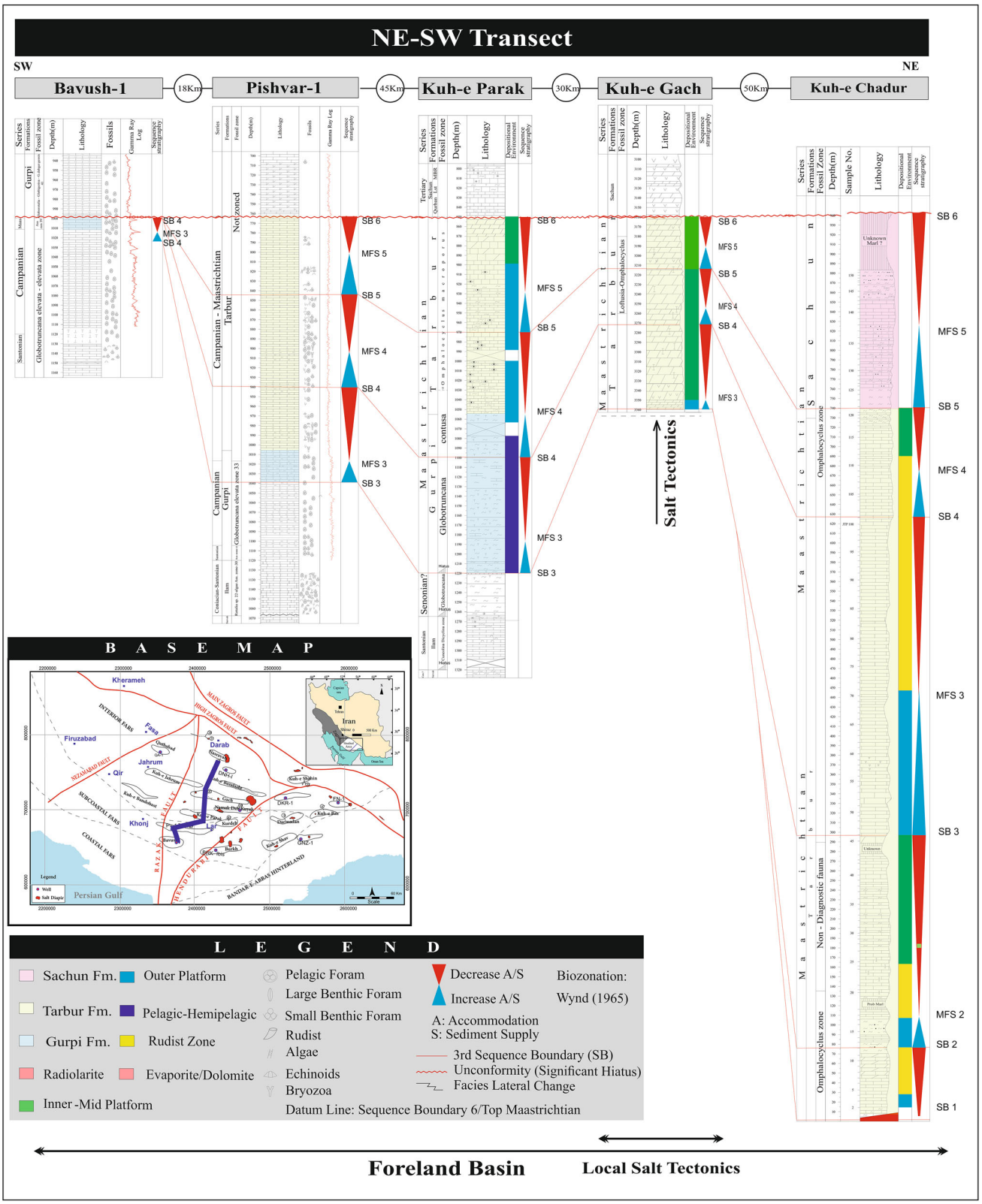

Fig. 14 Cross section with high-resolution sequence stratigraphy through the Maastrichtian deposits

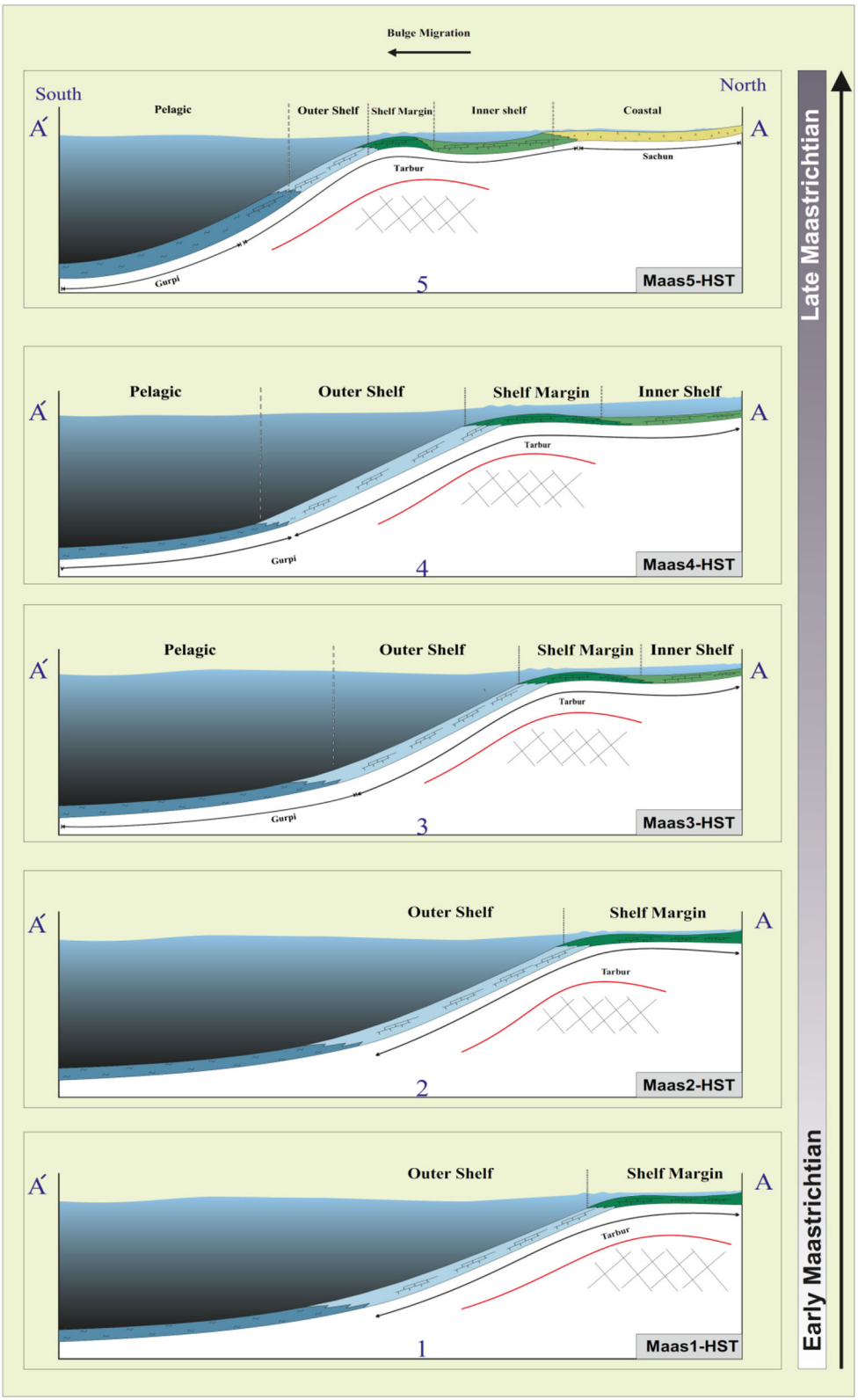

Fig. 15 Migration of mid-bulge from Maas-1 to -5 sequences during Maastrichtian time interval

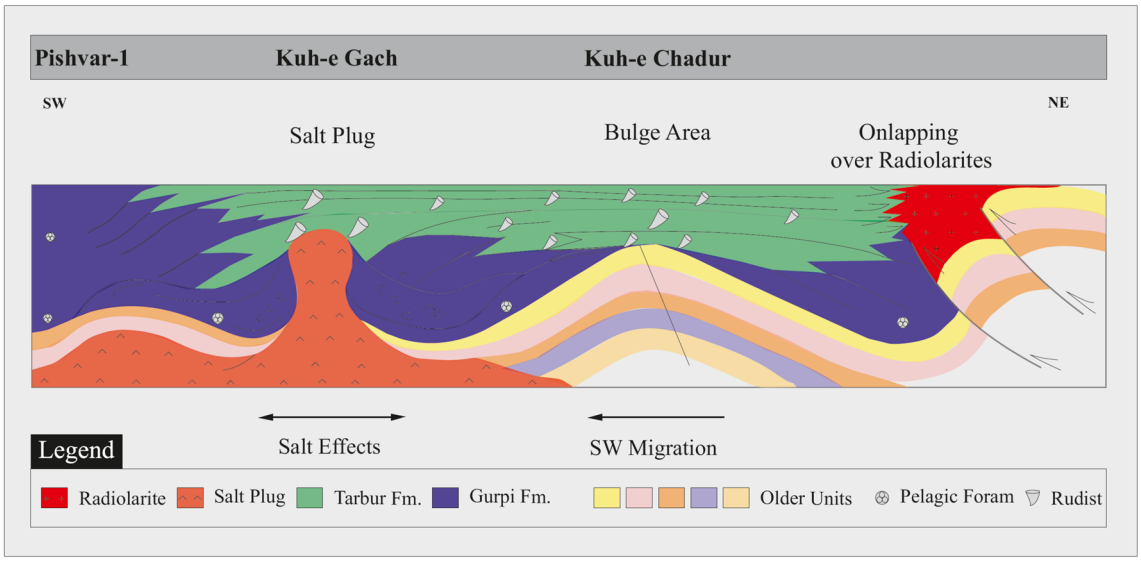

Fig. 16 Schematic tectono-sedimentary model of the Maastrichtian deposits in the eastern part of the Fars area

diagenetic processes play an important role particularly in recognizing the salt movements and related uplifted area.

Acknowledgements The author would like to thank National Iranian Oil Company, Exploration Directorate for providing data. We also thank the anonymous reviewers for their constructive comments of the first draft of the manuscript.

References

Abramovich S, Keller G (2002) High stress upper Maastrichtian paleoenvironment: inference from planktonic foraminifera in Tunisia. Palaeoclimatology 178:145–164

Abyat A, Afghah M, Feghhi A (2013) Stratigraphy and foraminiferal biozonation of the upper cretaceous sediments in Southwest Sepid Dasht, Lurestan, Iran. World Appl Sci J 28(9):1199–1207

Abyat A, Afghah M, Feghhi A (2015) Biostratigraphy and lithostratigraphy of Tarbur Formation (Upper Cretaceous) in southwest of Khoram Abad (southwest Iran). Carbonates Evaporites 30:109. doi:10.1007/s13146-014-0218-1

Afghah M, Yaghmour S (2014) Biostratigraphy study of Tarbur Formation (Upper Cretaceous) in Tang-e Kushk and East of Sarvestan (SW of Iran). J Earth Sci 25(2):263–274

Alavi M (2004) Regional stratigraphy of the Zagros fold-thrust belt of Iran and its Proforland evolution. Am J Sci 304:1–20

Alavi M (2007) Structures of the Zagros fold-thrust belt in Iran. Am J Sci 307:1064–1095

Amiri Bakhtiar H, Taheri A, Vaziri-Moghaddam H (2011) Maastrichtian facies succession and sea-level history of the Hossein-Abad, Neyriz area, Zagros Basin. Hist Biol 23(02–03):145–153. doi:10.1080/08912963.2010.498582

Asgari Pirbalouti B, Dehghanian MS, Rasti E (2012) Geochemical study of Late Cretaceous Sediments in Kuh-e Dezdaran Section, in Central Zagros of Iran. Adv Environ Biol 6(9):2541–2548

Asgari Pirbalouti B, Mirzaie M, Jafarian MA, Khosrow Tehrani K, Afghah M, Davoudi Fard Z (2013) Biostratigraphy and regional aspects of the Tarbur Formation (Maastrichtian) in Central Zagros, Southwest Iran. Ravista Italian di Paleontologia e Stratigrafia. 19(2):215–227

Bahroudi A, Koyi HA (2003) Effect of spatial distribution of Hormuz salt on formation style in the Zagros fold and thrust belt: an analogue modelling approach. J Geol Soc Lond 160:719–733

Catuneanu O, Galloway W, Kendall C, Miall A, Posamentier H, Strasser A, Tucker M (2011) Sequence stratigraphy: methodology and nomenclature. Newsl Stratigr 44:173–245

Catuneanu O, Martins NMA, Eriksson P (2012) Sequence stratigraphic framework and application to the Precambrian. Mar Petrol Geol 33:26–33

Dunham RJ (1962) Classification of carbonate rocks according to depositional texture. In: Ham WE (ed) Classification of carbonate rocks, vol 1. AAPG Memoir, pp 108–121

Embry AF, Klovan JE (1971) A Late Devonian reef tract on northeastern Banks Island, NWT. Bull Can Petrol Geol. 19:730–781

Emery D, Myers KJ (1996) Sequence stratigraphy. Blackwell Science, Oxford, p 297

Emery D, Flügel E (2010) Microfacies of carbonate rocks. Springer, New York, p 967

Farouk S (2014) Maastrichtian carbon cycle changes and planktonic foraminiferal bioevents at Gebel Matulla, West-Central Sinai, Egypt. Cretac Res 50:238e251

Farouk S, Jain S (2016) Benthic foraminiferal response to relative sea-level changes in the Maastrichtian-Danian succession at the Dakhla Oasis, Western Desert, Egypt. Geol Mag. doi:10.1017/S0016756816001023

Geel T (2000) Recognition of stratigraphic sequences in carbonate platform and slope deposits, empirical models based on microfacies analysis of palaeogene deposits in southeastern Spain. Palaeogeogr Palaeoclimatol Palaeoecol 155:211–238

Ghazban F (2009) Petroleum geology of the Persian Gulf. Tehran University Press. Tehran, Edition 2, p 707

Ghazban F, Al-Aasm IS (2010) Hydrocarbon-induced diagenetic dolomite and pyrite formation associated with the Hormoz Island salt dome, offshore Iran. J Petrol Geol 33(2):183–196

Haq BU, Hardenbol J, Vail PR (1988) Mesozoic and cenozoic chronostratigraphy and cycles of sea-level change. Soc Econ Paleontol Min Spec Publ 42:71–108

Harrison JV (1930) The geology of some salt plugs in Laristan. Q J Geol Soc Lond 86:463–522

Hesami K, Koyi HA, Talbot CJ (2001) The significant of strike-slip faulting in the basement of Zagros fold and thrust belt. J Petrol Geol 24(1):5–28

Hottinger L (1983) Processes determining the distribution of larger foraminifera in space and time. Utrecht Micropaleontol Bull 30:239–253

Hottinger L (1997) Shallow benthic foraminiferal assemblages as signals for depth of their deposition and their limitations. Soc Geol France Bull 168:491–505

Hottinger L (2007) Revision of the foraminiferal genus Globoreticulina Rahaghi, 1978, and of its associated fauna of larger foraminifera from the late Middle Eocene of Iran. Carnets de Géologie

Jahani S, Callot JP, De Lamotte DF, Letouzey J, Leturmy P (2007) The Salt Diapers of the Eastern Fars Province (Zagros, Iran). Springer, Berlin, pp 289–308

Jahani S, Callot JP, Letouzey J, de Lamotte DF (2009) The eastern termination of the Zagros Fold-and-Thrust Belt, Iran: structures, evolution, and relationships between salt plugs, folding, and faulting. Tectonics 28:22

Jamalian M, Adabi MH, Moussavi MR, Sadeghi A, Baghbani D, Ariyafar B (2010) Facies characteristic and paleoenvironmental reconstruction of the Fahliyan Formation, Lower Cretaceous, in the Kuh-e Siah area, Zagros Basin, southern Iran. Facies 57:101–122. doi:10.1007/s10347-010-0231-3

James GA, Wynd JG (1965) Stratigraphical nomenclature of Iranian Oil consortium agreement area. Am Assoc Petrol Geol Bull v49:2182–2245

Keller G (2012) The cretaceous–tertiary mass extinction, chicxulub impact, and Deccan volcanism. In: Talent JA (ed) Earth and life, international year of planet earth. Springer, Dordrecht, pp 759–793 doi:10.1007/978-90-481-3428-1_25

Kent PE (1958) Recent studies of south Persian salt plugs. AAPG Bull 42(12):2951–2972

Kent PE (1970) The salt diapirs of the Persian Gulf region. Leic Lit Philos Soc Trans 64:55–58

Kent PE (1979) The emergent Hormuz salt plugs of southern Iran. J Petrol Geol 2(2):117–144

Koop WJ, Stoneley R (1982) Subsidence history of the Middle East Zagros Basin, Permian to recent. Philos Trans R Acad Soc Lond A 305:149–168

Mehrabi H, Rahimpour-Bonab H, Hajikazemi E, Jamalian A (2015) Controls on depositional facies in Upper Cretaceous carbonate reservoirs in the Zagros area and the Persian Gulf, Iran. Facies 61:23. doi:10.1007/s10347-015-0450-8

Miall AD (2000) Principle of sedimentary basin analysis. Springer, New York, p 616

Moro A, Skelton PW, Cosovic V (2002) Palaeoenvironmental setting of Rudists in the Upper Cretaceous (Turonian-Maastrichtian) Adriatic carbonate platform (Croatia), based on sequence stratigraphy. Cretac Res 23:489–508

Mosadegh H, Shirazi M (2009) Algal biozonation of Fahliyan Formation (Neocomian) in the Zagros Basin, Iran. European Geoscience Union. Geophys Res Abst EGU2009-8507 11:1

Motamedi H, Sepehr M, Sherkati S, Pourkermani M (2011) Multiphase Hormuz salt diapirism in the southern Zagros, SW Iran. J Petrol Geol 34(1):29–44

Motiei H (1993) "Stratigraphy of Zagros," treatise on the geology of Iran, geological survey of Iran, p 536

Motiei H (1995) Stratigraphy of Zagros. Publ. Geol. Survey of Iran (in Farsi), pp 536

Ozcan E (2007) Morphometric analysis of the genus Omphalocyclus from the Late Cretaceous of Turkey: new data on its stratigraphic distribution in Mediterranean Tethys and description of two new taxa, Cret. Research 28:621–641

Palma RM, Lopez-Gomez J, Piethe RD (2007) Oxfordian ramp system (La Manga Formation) in the Bardas Blancas area (Mendoza Province) Neuquen Basin, Argentina: facies and depositional sequences. Sediment Geol 195:113–134

Piryaei A, Reijmer JJG, Vanbuchem FSP, Yazdimoghadam M, Sadouni J, Danelian T (2010) The influence of Late Cretaceous tectonic processes on sedimentation patterns along the north-eastern Arabian plate margin (Fars Province, SW Iran). In: Leturmy P, Robin C (eds) Tectonic and stratigraphic evolution of Zagros and Makran during the Mesozoic-Cenozoic. Geol. Soc. Lond. Spec. Publ., pp 330

Piryaei A, Reijmer J, Borgomano J, van Buchem F (2011) Late Cretaceous tectonic and sedimentary evolution of the Bandar Abbas Area, Fars region, southern Iran. J Petrol Geol 34(2):157–180

Player RA (1967) A note on the Fars Salt Plugs. Iranian Oil Operation Companies. Geological exploration and production division. Unpublished Report

Purser BH (1973) The Persian Gulf: holocene carbonates sedimentation and diagenesis in a shallow epicontinental sea. Springer, Berlin, p 471

Riding R (1991) Calcareous algae and stromatolites. Springer, Berlin

Sepehr M, Cosgrove JW (2005) Role of the Kazerun fault zone, in the formation and deformation of the Zagros fold thrust belt, Iran. Tectonics 24(5). doi:10.1029/2004TC001725

Setudenia A (1978) Mesozoic sequence in South West Iran and adjacent area. J Petrol Geol 1(1):3–42

Sharland P, Archer D, Casey R (2001) Arabian plate sequence stratigraphy. Blackwell, Oxford, p 320

Sherkati S, Letouzey J (2004) Variation of structural style and basin evolution in the central Zagros (Izeh zone and Dezful Embayment), Iran. Mar Petrol Geol 21(5):535–554

Talbot C, Alavi JM (1996) The past of a future syntaxis across the Zagros. In: Alsop GL, Blundell DL, Davison I (eds) Salt tectonics. Geological Society, London, Special Publications, vol 100, pp 129–151

Tucker M (1993) Carbonate diagenesis and sequence stratigraphy. In: Wright VP (ed) Sedimentology review. Blackwell, Oxford, pp 57–72

Tucker ME, Wright VP (1990) Carbonate sedimentology. Blackwell. Sci. Pub., pp 482

Vail P (1991) The stratigraphic signatures of tectonics, eustasy and sedimentology: an overview. Springer, Berlin, pp 617–659

van Buchem FSP, Pittet B, Hillgärtner H, Grötsch J, Al Mansouri AI, Billing IM, Droste HHJ, Oterdoom WH, van Steenwinkel M (2002) High-resolution sequence stratigraphic architecture of Barremian/Aptian carbonate systems in Northern Oman and the United Arab Emirates (Khairab and Shu'aiba Formations). GeoArabia 7:461–500

van Buchem FSP, Baghbani D, Lg Bulot, Caron M, Gaumet F, Hosseini A, Immenhauser A, Keyvani F, Schroeder R, Vedrenne V, Vincent B (2006) Aptian Organic-rich Intrashelf Basin Creation in the Dezful Embayment (Kazumi and Dariyan Formations, SW Iran). AAPG meeting Houston, Houston

van Wagoner JC, Posamentier HW, Mitchum RM, Vail PR, Sarg JF, Loutit TS, Hardenbol J (1988) An overview of the fundamentals of sequence stratigraphy and key definitions. In: Wilgus CK, Hastings BS, Kendall CG. St. C, Posamentier HW, Ross CA, Van Wagoner JC (eds) Sea-level changes: an integrated approach. Society of economic paleontologists and mineralogists, Special publication no. 42, pp 39–45

Wilson JL (1975) Carbonate facies in geologic history. Springer, New York, p 439

Wynd JG (1965) Biofacies of the Iranian oil consortium agreement area. Report 1082, Iranian Oil Operating Companies, Geological and Exploration Division, Tehran